MODELING BINDER REMOVAL IN CERAMIC COMPACTS

By

MATTHEW L. INCLEDON

A thesis submitted to the

Graduate School-New Brunswick

Rutgers, The State University of New Jersey

in partial fulfillment of the requirements

for the degree of

Master of Science

Graduate Program in Materials Science and Engineering

written under the direction of

Professor M. John Matthewson

and approved by

_____

_____

_____

New Brunswick, New Jersey

May, 2013

ABSTRACT OF THE THESIS

Modeling Binder Removal in Ceramic Compacts

By MATTHEW L. INCLEDON

Thesis Advisor: Prof. M. John Matthewson

Binder is often added to ceramic systems to provide mechanical strength to the green bodies during processing. The binder removal sequence for an individual system is difficult to predict due to the thermal reaction and mass transport of the volatile products. The objective of this work is to use computational methods to predict the kinetics of binder removal as a function of composition, particle size, pore size and tortuosity, temperature, body size and shape, *etc.*. The model will be used to predict the composition, temperature, and pore pressure as a function of time, position within the body, and heating sequence parameters. This will provide the ability to predict optimum heating sequences that minimize processing time and energy input while avoiding harmful high internal pressures and temperatures. Since there are many binder systems in use, a few specific cases will be considered. TGA (thermogravimetric analysis) of binders will be used to measure kinetics parameters that are inputs for the computational model.

A framework will be developed to assess the binder removal sequence for a binder and ceramic system. The input for the model, computed in COMSOL Multiphysics, will be determined through analysis of TGA weight loss data and green body characterization.

A set of tools will be presented that assist in the fitting of the TGA data, including the binder degrading into multiple species, higher order reactions, parallel and series reactions, *etc..* The use of these ideas and tools will allow the modeler to better predict the heating sequence required for a ceramic and binder system to successfully remove all binder material.

Table of Contents

List of Tables

viii

1. Introduction

1.1 Ceramics

The use of ceramics dates back to before 5000 BC when inhabitants were hand mixing and forming material from the earth and allowing it to dry into a hardened state. Today's field of ceramics includes corrosion-resistant silicon carbide components for chemical processing, alumina structural ceramics for technology and electronic application, and silicate ceramic products such as porcelain, among many others. From the rudimentary processes of molding clay to obtain a cup for drinking water to today's methods such as spark plasma sintering for fiber reinforced ceramics, ceramics are constantly being researched and improved.[6] The advance of technology is an even greater stimulus to improve materials. Old materials are getting second looks and being reinvented as future materials at the same time that new materials are being discovered.[7]

The processing of ceramics has become a science. A final ceramic product is influenced by each stage of the process. Variations in the processing procedure will yield different results. The materials and operations require careful oversight to ensure consistency. Therefore, the objective of process engineering is to change the important characteristics of the process to improve the product quality and efficiency of production.[6] The success in optimizing the production sequence for ceramics begins with the processing procedure.

A ceramic begins with the mixing of a single or multiple powders and/or liquids. These raw materials are chosen based upon material cost, market factors, vendor services, technical processing considerations, and the ultimate performance requirements and market price of the finished products.[6] A detailed analysis of processing procedures has

been discussed in reference 6. Once the desired powders and liquids have been selected, they are subject to a shaping method: dry pressing, injection molding, extrusion, roll compaction, tape casting, pressure casting, or slip casting.[8] The shaped ceramic is eventually heated in an oven for sintering. Sintering is the consolidation of the product; the particles have joined together into an aggregate that has strength, which may or may not include densification and shrinkage. Typically, sintering temperatures exceed one-half to two-thirds the melting temperature, which range from 1150°C - 1700°C for most ceramics.[6]

1.2   Binder

In many ceramic processing settings, an interim stage exists between shaping and sintering. The shaped, unfired ceramic, or green body, undergoes stress in the form of testing, machining, and transporting, among other things. Since this stress makes the green body susceptible to mechanical failure, additional raw materials, binders, may be added to the ceramic system to ensure strength of the green body. Aside from the primary function of improving green strength, binders can also be added as a wetting agent, thickener, suspension aid, rheological aid, body plasticizer, liquid retention agent, and consistency aid.[6] Binders are chosen based on certain criteria such as easy removal, strong adhesion to powder, cohesive strength, solubility in fluidizing liquid, and low cost.[8]

While the addition of binder to a green body is beneficial to its green mechanical strength, the binder cannot be present in the green body during final sintering. The presence of binder during final sintering can give rise to defects in the final ceramic product and therefore must be removed prior to final sintering. The removal of the binder occurs

as the binder is heated to a temperature that allows liquid diffusion or gas-phase diffusion. As the melting temperature of the binder is reached and it begins to vaporize, the volatile products transport through the porous media out of the body.

The binder removal process presents challenges to the manufacturer of the product. Ideally the binder is completely removed as quickly as possible. The binder must navigate the porous media in order to escape the body. If volatile species are produced faster than the green body's porous pathways allow for mass transport, internal pressure will buildup and ultimately lead to failure at a critical pressure. Therefore, the heating sequences for binder removal must be slow enough to stay below the critical pressure threshold but fast enough to justify the use of binders. Yet, as each ceramic system is different and binders can take the form of many different materials, the interaction between binder degradation and mass transport through the porous body is difficult to predict.

1.3   Binder Removal Model

The current approach to binder removal is based on previous knowledge and weight loss data to give a first approximation at the removal sequence. This is inefficient due to its consumption of time, materials, and energy. The ability to model the binder removal process would benefit those manufacturing ceramic systems using binder.

1.4   What is Modeling?

A model is a tool used to study the behavior of a complex system without the need for physical experimentation. An accurate model is developed by linking all of the physical processes occurring in the system and encompassing all of the effects that each

process may have on other parts of the system. More specifically, computational modeling is a method of modeling many operations at once, repetitively, without the need to carry out the work by hand. The use of a computer to carry out calculations greatly increases the scope of phenomena that can be modeled. In the case of binder removal a numerical model is employed. A numerical model is an iterative method that calculates a system's values for a specified step, typically in time. Numerical models are used when an analytical solution is not easily obtained. Therefore, the more computing power that is available the more numerical solutions to several thousand simultaneous linear algebraic equations in a few minutes, since the time steps between calculations can be smaller.[9]

When modeling binder removal, a partial differential equation (pde) is being solved. Since we do not apply any simplifying assumptions to simply obtain an analytical solution, we must numerically solve the pde. What does this mean? Suppose one wants to track the evolution of the binder in a ceramic body after ten seconds at a constant heating rate. For simplicity, we assume all of the necessary parameters regarding the system are known, with a set of initial conditions. Taking a time step of one second, one would calculate the pressure after one second and re-calculate all of the variables at the new time (gas in the body increases, binder volume decreases, temperature increases, *etc*.). This would be done after two seconds, three seconds, *etc*., until ten seconds is reached. If a powerful computer is carrying out the calculations, the time step could be decreased to a tenth of a second, which would provide even more accurate results. Smaller time steps yield more accurate results for two reasons. The calculations at each step are dependent on the solutions of the previous time step and the

physical processes occurring are continuous, so the closer one can get to a continuous time-step, the more accurate the numerical model will be.

The allure of modeling ceramics processing is to determine the most efficient way to manufacture a product by keeping its integrity intact but cutting down on time and materials. Today's standard for determining binder removal sequences is a rudimentary method of trial-and-error. If pieces are breaking using the current heating sequence or the sintering process is failing, the manufacturer will simply use a slower heating rate or add in some temperature holds. At the end of the day, this is an inefficient way to produce ceramics. This guess-and-check method wastes materials and simply finds a heating sequence that "works," opposed to finding the best heating sequence. In a proper model of the binder removal sequence, parameters of the system will be taken in as parameters. Once the fracture strength of the green body is determined, various heating rates and hold times can be simulated to find the optimal sequence heating environment, staying below the critical internal pressure.

1.5   Modeling and Experimental Work

The goal of this project is to develop a model that can assist in optimizing a binder removal sequence with minimal experimentation. Each step in the production of a ceramic is dependent on the quality of the preceding processing steps. When the processing sequence reaches the stage of a green body, all of the work done to get the powder to that state is irreversible. The person responsible for removal of the binder simply knows the parameters of their piece, which are a result of how the piece was prepared, and that the body must be devoid of all binder material. The goal of this

research is to provide a tool to allow execution of binder removal processing as thoroughly and efficiently as possible.

Various ceramic systems could be analyzed in the model based on the system's parameters such as porosity, percent binder, percent ceramic powder, tortuosity, *etc.*. Rather than re-invent the wheel, we propose to use knowledge developed from past literature to develop a model from the ground up.

The first task to modeling the binder removal in a ceramic system is to understand all of the working components of the phenomenon. The main processes are the thermal reaction of the binder and the mass transport of the volatile products from the reaction.

1.6 Reaction

A majority of the binders used for advanced ceramics systems are polymers. Polymers are materials that have a very large molecular structure, typically chain-like with repeating units. If the polymer is an organic compound it has a backbone chain of carbon atoms. Polymers usually have low densities and are ductile and pliable.[10] We are interested in removing the polymer from the porous green body, which is accomplished by thermal degradation. Therefore, it would be useful to understand the thermal degradation process in polymers.

A typical organic polymer consists of a carbon backbone that has repeating side groups coming off of the carbon chain. The number of repeating backbone/side-group segments can change and will give the polymer a different molecular weight, thereby modifying its characteristics. The number of unique side groups, their complexity, their bond strength, *etc.*, determine how the thermal degradation proceeds. Multiple

mechanisms exist that cause a material to degrade, and the prominent mechanisms in polymer degradation are random-chain scission, end-chain scission, cross-linking, and chain stripping. In random-chain scission, degradation occurs at random locations in the chain. With end-chain scission, individual monomer units are removed at the chain end. Chain-stripping involves atoms not part of the chain getting cleaved and cross-linking creates bonds between polymer chains.[11]

As is often the case, a polymer does not degrade into a volatile form in a single step. The polymer may undergo a series of reactions at successive temperatures, further breaking down the polymer at each reaction. An example of this reaction is displayed in Figure 1.

$$\text{Polymer} \xrightarrow{k_1} \text{Solid}_1 + \text{Gas}_1 \qquad \text{Solid}_1 \xrightarrow{k_2} \text{Solid}_2 + \text{Gas}_2$$

Figure 1. Diagram showing polymer degradation in more than one step.

In this diagram, the degradation of the polymer into an intermediate solid and a gas occurs at a lower temperature than the degradation of the intermediate solid to a gas. The weight loss profile of this reaction would have at least two regions of rapid weight loss since the gases are produced at different temperatures, which are described by their reaction rates, k_1 and k_2, respectively.[12]

The physics behind polymer degradation present a challenge to the modeler. Given this degradation phenomenon, it is not unusual for ceramics manufacturers to add a variety of polymer types, such as multiple molecular weights and binder species, to a ceramic system. This ensures that the polymers break down at different temperatures so all of the volatile gas is not trying to escape from the body at once. A single polymer degradation

scenario would be highly susceptible to fracture due to internal pressure buildup. Yet, a multiple binder system is much more difficult to model than a single binder system, which is itself a challenge to model if it has multiple species breaking off at different times.

1.7   Literature Review

A significant amount of literature exists on the topic of modeling binder removal. Particularly, Stephen Lombardo's group out of the University of Missouri has published significant work on modeling binder removal. Three of Lombardo's papers in particular[1,13,14] each focus on a specific effect of binder decomposition but follow the same theoretical model regarding removal.

In Reference 14, a model is developed to determine under which conditions removal proceeds as a planar-front and which conditions necessitate homogenous removal. Planar-front removal assumes the binder decomposition occurs at the outer edges of the body and recedes as a planar front into the body in time, as presented in Figure 2. As temperature increases and a gradient is introduced in the body, the binder closer to the boundary of the body will reach its volatization temperature sooner than the binder that is closer to the centerline of the body.
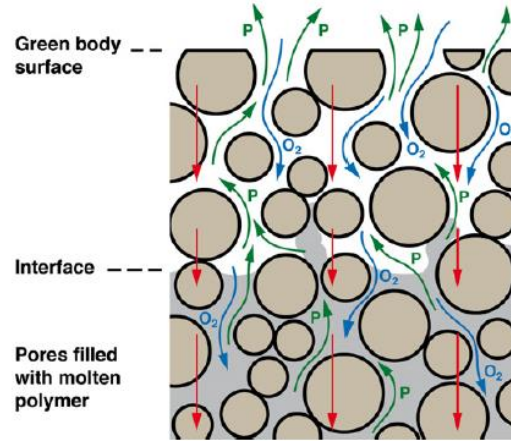
Figure 2: Diagram[2] representing planar-front binder removal model as temperature is increased.

Homogenous removal involves uniform degradation of the binder throughout the body in time. This is displayed in Figure 3. In the case of homogenous removal, a temperature gradient does not exist throughout the body allowing for the binder to reach its volatization temperature uniformly.

In Reference 14, a model is developed to simulate the removal of binder from injection-molded ceramics components, which considers heat transfer, mass transfer, and reaction kinetics. Using the model, it is concluded that planar-front removal occurs with high thermal resistance, specifically when $L^2/\alpha \geq 10^4 \, s$, where L is the body half-thickness and α is the thermal diffusivity. Homogenous binder removal occurs below this value.
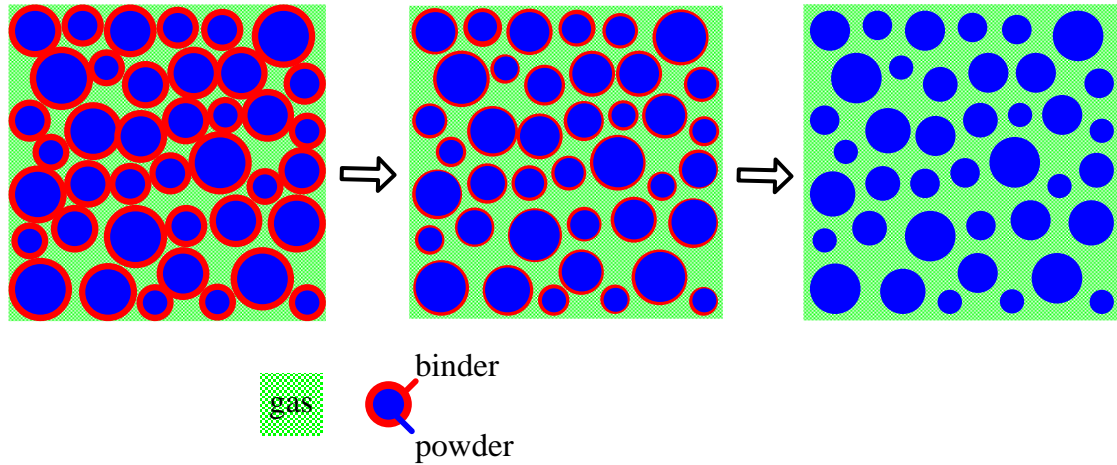
Figure 3: Diagram representing homogenous binder removal as the body heats up.

Liau's paper on determining the effect of body geometry on pressure buildup and the catalytic effects of metal electrodes in a multilayer capacitor during burnout[13] uses the same theory to develop a model for the pressure buildup within the body during binder burnout. The same holds true in Shende's paper on determining the decomposition kinetics parameters of the binder during removal[1].

1.8   Degradation Kinetics Determination

Lombardo's group derives an expression[1,13,14] for the internal pressure buildup in the ceramic body during debinding in the follow manner. A model that describes the removal of binder from a ceramic green body must account for polymer decomposition, reaction kinetics, and mass transport. The following assumptions are made in the comprehensive model involving these processes:

- Conduction is the only mode of heat transfer in the green body (heat of reaction and convective heat transfer are negligible)

- Thermal diffusivity does not vary with temperature

- Binder burnout decomposition kinetics are determined on a per-species basis, but the products are all gases

- Darcy's Law is used to describe the gas flow of decomposition products out of the body, (assumed when the pore size is large relative to the mean free path of the gas-phase species, used here because this is the case of slower transport and therefore larger internal pressure being the rate limiting factor)[14]

Shende and Lombardo[1] assume a simple and irreversible process, where a single species binder material, B, has a single reaction path,

$$B \rightarrow \text{products.} \tag{1}$$

While TGA (thermogravimetric analysis) directly measures the mass of the binder, Shende and Lombardo[1] cast their model in terms of the volume of binder, where the fraction of binder reacted is:

$$\alpha = \frac{V_0 - V_b}{V_0}, \tag{2}$$

where V_0 is the initial volume fraction of binder and V_b is the volume fraction of binder that remains at time, t. The rate of binder reacted as a function of time is expected to be a function of how much binder remains, which itself is some function, f, of the amount reacted:

$$\frac{d\alpha}{dt} \propto f(\alpha). \tag{3}$$

This function might take several forms, for example a classic first order reaction where $f(\alpha) = (1-\alpha)$ or an nth order reaction where $f(\alpha) = (1-\alpha)^n$. The choice of the particular

form of $f(\alpha)$ to use is based on the quality of fit of the model to experimental data. Shende and Lombardo opt for a first order reaction for simplicity:

$$\frac{d\alpha}{dt} = k(1-\alpha).$$ (4)

The proportionality constant in Equation (4) is the rate constant, k, which is assumed to have Arrhenius temperature dependence:

$$k = A\exp\left[-\frac{E}{RT}\right],$$ (5)

where E is the effective activation energy, R is the gas constant, and T is the absolute temperature.

Typically, Equation (4) can be simply integrated at constant temperature to obtain how α develops in time. However, a linear heating rate is modeled:

$$\beta = \frac{dT}{dt},$$ (6)

so that k is not a constant in Equation (4) and therefore cannot be integrated analytically. Lee and Beck[3,3] describe an approximate method for integration of Equation (4) that results in a fractional error on the order of RT/E, (i.e. is valid for $E \gg RT$, which is typically the case). Lee and Beck's method involves considering the integral of the function f:

$$F(\alpha) = \int_0^\alpha f(\alpha')\, d\alpha'.$$ (7)

Their approximation leads to:

$$\ln\left[\frac{F(\alpha)}{T^2}\right] = \ln\left[\frac{AR}{\beta(E+2RT)}\right] - \frac{E}{RT}.$$ (8)

If the reaction is first order, $f(\alpha) = (1-\alpha)$ and $F(\alpha) = -\ln(1-\alpha)$, leading to:

$$\ln(1-\alpha) = \frac{-ART^2}{\beta(E+2RT)}\exp\left[-\frac{E}{RT}\right]. \tag{9}$$

The parameters E and A are found by plotting $\ln(1-\alpha)$ against temperature and fitting

Equation (9) to the result. Thermogravimetric Analysis (TGA) measures the weight loss

of a sample subject to a constant heating rate. As species in the sample degrade and volatile

species escape, a balance tracks the weight loss throughout the time of the temperature

ramp. The TGA data collected by Shende and Lombardo for a PVB-BaTiO$_3$-Pt (polyvinyl

butyral binder, barium titanate ceramic, and platinum electrodes) composition is presented

in Figure 4.
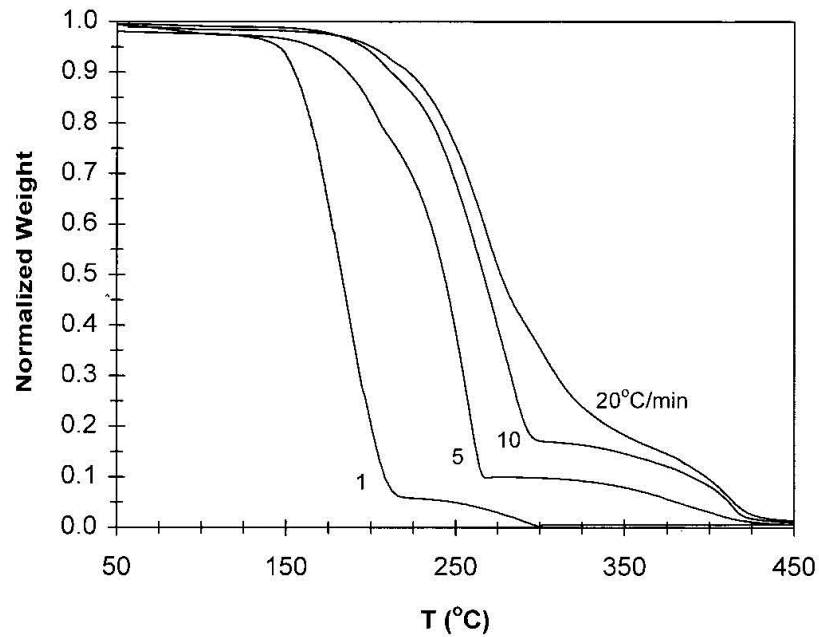
Figure 4: TGA data[1] are from Shende and Lombardo, showing the weight loss profile that is used to determine the kinetic parameters. Data is for a PVB-BaTiO$_3$-Pt composition.

Dirion et al.[12] takes the determination of degradation kinetics one step further by

assuming more than a single species is produced from the polymer degradation and

therefore more than one reaction is taking place. This necessitates an A and E for each

reaction. These parameters can be found in a similar manner to the method above, by fitting to equation (9). Yet, Dirion *et al*. propose to couple the different stages of degradation by creating a degradation flow chart, similar to Figure 1, and extracting the weight loss rates for each stage of decomposition. The rates from Figure 1 would look as follows:

$$\frac{dy_p}{dt} = -k_1 y_p = -A_1 e^{-E_1/RT} y_p$$

$$\frac{dy_{S1}}{dt} = -a\left(k_1 y_p - k_2 y_{S1}\right) = -a\left(A_1 e^{-E_1/RT} y_p - A_2 e^{-E_2/RT} y_{S1}\right)$$

$$\frac{dy_{S2}}{dt} = bk_2 y_{S1} = bA_2 e^{-E_2/RT} y_{S1}$$

$$z = y_p + y_{S1} + y_{S2}$$

Figure 5. Rate equations for three species reacting and their normalized weight loss.

In these rate equations, *y* represents the normalized weight of each species and *z* represents the total normalized weight of the body.

Immediate inspection of Figure 4 raises some skepticism regarding the weight loss behavior. Traditionally, Arrhenius behavior causes weight loss to occur earlier in the temperature sequence as the heating rate is increased. From the data in Figure 4, the opposite behavior occurs. This makes it nearly impossible to develop a model with a single set of kinetics parameters that fit all of the data if an Arrhenius activated process is being modeled.
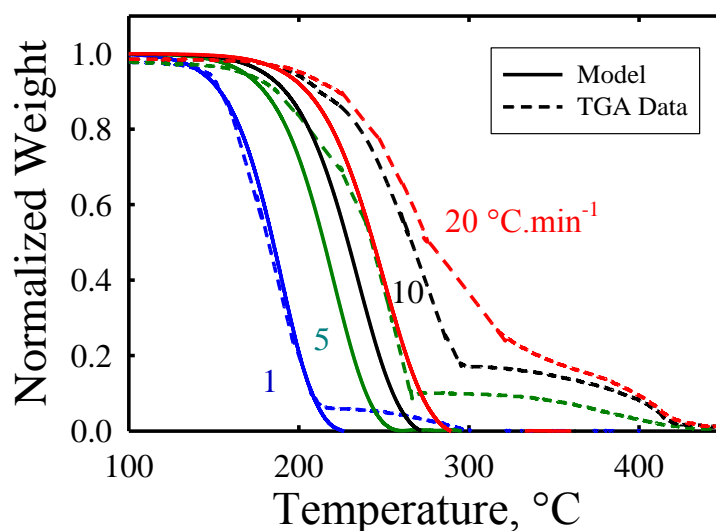
Figure 6: Shende and Lombardo's model[1] fitted to their TGA data for a PVB-BaTiO$_3$-Pt composition, showing how the first order, single species assumption gives poor agreement. The kinetic parameters are for $\beta = 10°C \cdot min^{-1}$.

When the TGA data are fit with Lee and Beck's Integral method,[3] it becomes more apparent that the fit used by Shende and Lombardo does not properly describe the data. Figure 6 compares the TGA data with the fit for each heating rate using the kinetics parameters for a heating rate of 1 °C·min^{-1}.

It is apparent in Figure 6 that Shende's single species model agrees well with the first weight loss region of the experimental data for the same heating rate, but those parameters do not transfer well to the other experimental heating rates. Considering the cause of the second weight loss region, Fourier Transform Infrared Spectoscopy (FTIR) data from this sheds some light. The FTIR absorbance spectra are presented in Figure 7, where two regions of time exhibit significant absorbance.
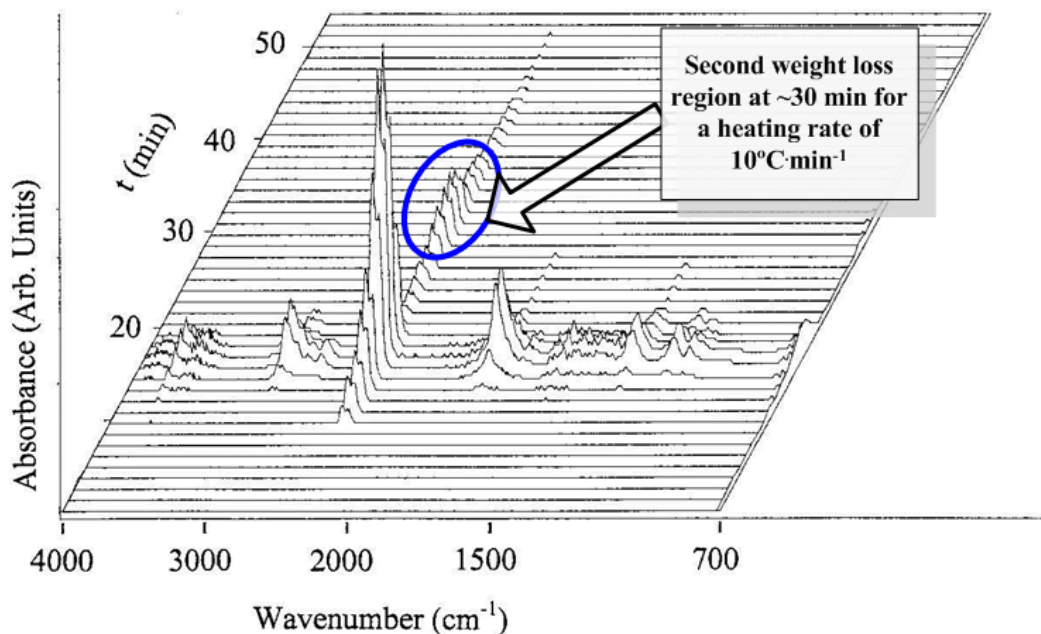
Figure 7: Shende's FTIR absorbance spectra[1] for a PVB-BaTiO$_3$-Pt composition with $\beta = 10°C \cdot \min^{-1}$. Multiple weight loss regions are apparent.

The first region occurs at 12-20 minutes, which with a starting temperature of 27 °C, is around 150-220 °C, and the second region starts ~30 minutes, ~320 °C. Considering the PVB must transport out of the body after it reacts, the FTIR absorbance spectra indicates that there are more than a single species volatizing throughout the binder degradation.

1.9   Internal Pressure Expression Derivation

Liau investigates a multilayer capacitor (MLC) with moderate binder loading and determines that the main transport mechanism is gas-phase convection.[13] This conclusion is drawn based on the high velocity of gases evolved. If the migration of the binder were greater, the reaction kinetics would be constant as opposed to first order, in which case the velocity of gas exiting the body would not be so high. This leads Liau to consider the escape of binder as gas flow in porous media, which has the following continuity equation

$$\frac{\partial\left(V_g\rho\right)}{\partial t} = -\frac{\partial}{\partial x}\left(\rho u\right) + \frac{r(x,t)}{M}, \tag{10}$$

where $V_g = 1 - V_s - V_b$ is the porosity within the body, V_s is the volume fraction of ceramic in the green body, ρ is the molar gas density, $r(x,t)$ is the reaction rate as described by equation (4), and M is the average molecular weight of the gas-phase products. The left hand side of equation represents the amount of gas at time, t, and the right hand side is the creation of gas (second term) minus the diffusion of binder to the surface of the green body (first term). The superficial velocity, u, is the volume flow rate in a porous media assuming no other media is flowing in that cross-sectional area. The superficial velocity is represented by Darcy's Law:

$$u = -\left(\frac{\kappa}{\mu}\right)\frac{\partial p}{\partial x}, \tag{11}$$

where μ is the viscosity of the gas, p is the local internal pressure of the ceramic body, and κ is the permeability of the gas in the pore space, which is represented by:

$$\kappa = \frac{V_g^3}{k\left(1-V_g\right)^2 S^2}, \tag{12}$$

The constant that accounts for the shape and tortuosity of the pores is k and S is the surface area per unit volume of the body.

Shende solves the continuity equation analytically by using assumptions to simplify some of the coupled processes. Through simulations of temperature and binder volume throughout the body, Shende determines that the gradients are close enough to zero that they do not affect the solution for the buildup of pressure within the body, so

$\partial T / \partial x = 0$ and $\partial V_b / \partial x = 0$, which alludes to a homogenous removal model. The third

assumption made is a pseudo-state assumption, $\dfrac{\partial}{\partial t}(V_g \bar{\rho}) = 0$, where $\bar{\rho} = pRT_0 / P_0$. This

assumes that the model is only dealing with the slow reactions and allows for the

reactions to reach a steady state per each time step of the model.

These simplifying assumptions lead to an analytical solution for the relative

pressure buildup along the centerline of the body[1]:

$$\left(\frac{P}{P_0} \right)_{centerline} = \left[1 + \frac{\mu k S^2 RT}{MP_0^2} \frac{\left(1 - V_g\right)^2}{V_g^3} r(x,t) L^2 \right]^{1/2} . \tag{13}$$

We believe that making these simplifying assumptions detracts from the accuracy

of the model and limits the scope of analysis when compared to the experimental results.

Rather, we do not make any simplifying assumptions and solve for the pressure buildup

within the model numerically. COMSOL Multiphysics, a finite-element package, is used

to carry out the analysis. This software allows us to look at different geometries and focus

on various physical processes occurring simultaneously during the reaction process.

Lastly, the continuity equation (10) is limited to a single reaction species. Considering the

kinetics parameters that Shende fits to the experimental data do not fit properly, we modify

this continuity equation and solve for more than a single species volatizing during the

reaction and transporting out of the body. Multiple species leads to multiple reactions,

which we model in parallel (multiple reaction paths) or in series (sequential reaction path).

2.   Physics of the Reaction

2.1   Determining Reaction Kinetics

In order to model the internal pressure in a green body the reaction kinetics of the system must be known. From first principles, the rate of reaction of material is the change in amount of material at the reaction site per interval of time. The amount of material can be measured in terms of mass:

$$r_i = \frac{dm_i}{dt}, \tag{14}$$

where r_i is the reaction rate of material i and m_i is the mass of material i. The reactions encountered in binder removal produce solid, liquid, or gas from the solid binder. Therefore, since multiple phases are encountered in these reactions, they are considered heterogeneous reactions.[15]

For open porosity systems, the heating of the green body will occur in an inert atmosphere so that conduction of heat through the body will cause the reaction to occur. In systems with closed porosity a gas such as air may be used to react with certain components of the system, causing degradation and volatile transport.

To simplify the reaction to account for both heterogeneous reaction and weight loss throughout the body, the mass can be normalized. Since the original mass will stay constant:

$$r_i = \frac{1}{m_{i,0}} \frac{dm_i}{dt} = \frac{dy_i}{dt}, \tag{15}$$

where $y_i = m_i / m_{i,0}$ is the normalized mass of species i. In a heterogeneous reaction, the rate of reaction is expected to take the following form:

$$r_i = f\left(\text{activities}\right) = k y_i^{n_i}, \tag{16}$$

Where k is the rate constant (varies with temperature) of the reaction and n is the order of reaction. The reaction order n is determined by method of best fit, which has been verified experimentally for many reactions of interest. The rate constant, k, typically takes the form of an Arrhenius equation, as seen in Equation (5).

To determine the reaction kinetics from weight loss data, the reaction rate must be fit to the weight loss data to determine the constants A and E. The reaction equation can be fit by recalling that $\beta = dT/dt$ and rearranging as follows:

$$r = \frac{dy_i}{dT} = \frac{A}{\beta}\exp\left[-\frac{E}{RT}\right]y_i \quad \rightarrow \quad \frac{dy_i}{y_i} = \frac{A}{\beta}\exp\left[-\frac{E}{RT}\right]dT. \qquad (17)$$

The right hand side of equation (17) cannot be integrated analytically. Therefore, it is integrated by parts to obtain the following solution[3]:

$$F(y_i) = \frac{T^2 AR}{\beta(E+2RT)}\exp\left[\frac{-E}{RT}\right], \qquad (18)$$

where $F(y_i)$ is the integrated form of y_i. If the reaction is assumed first-order, from (16) the normalized mass takes the form y_i^1, then (18) can be rearranged:

$$\ln(y_i) = \frac{T^2 AR}{\beta(E+2RT)}\exp\left[\frac{-E}{RT}\right]. \qquad (19)$$

To fit (19) to TGA weight loss data, the data must first be normalized with respect to the binder weight. The natural log of the normalized binder weight plotted against the temperature can then be fit using (19) through the Matlab function Ezyfit.[16]

This method of curve fitting is presented in the following example corroborating Shende's heating parameters[1] using the integral method at a heating rate of 1°C·min⁻¹. Shende's weight loss data from Figure 4 were digitized and plot as $-\ln(1-\alpha)$ vs. T [K]. Figure 8 shows the fit and the associated parameters were determined as

$A = 7.681 \times 10^6 \text{ s}^{-1}$ and $E = 82.33 \text{ kJ·mol}^{-1}$. These values do not fall within reasonable

agreement of Shende's values of $A = 2.34 \times 10^7 \text{ s}^{-1}$ and $E = 92.5 \text{ kJ·mol}^{-1}$. This is attributed

to Shende's access to accurate and likely vast number of experimental data points opposed

to our method of digitizing data from a rather small plot from a journal. Shende fit data

corresponding to a normalized weight of 0.96-0.09. While we attempted to fit data within

the same range, the data that we were able to digitize did not produce many data points;

therefore, this range was estimated (~0.96-0.07) and not precise.
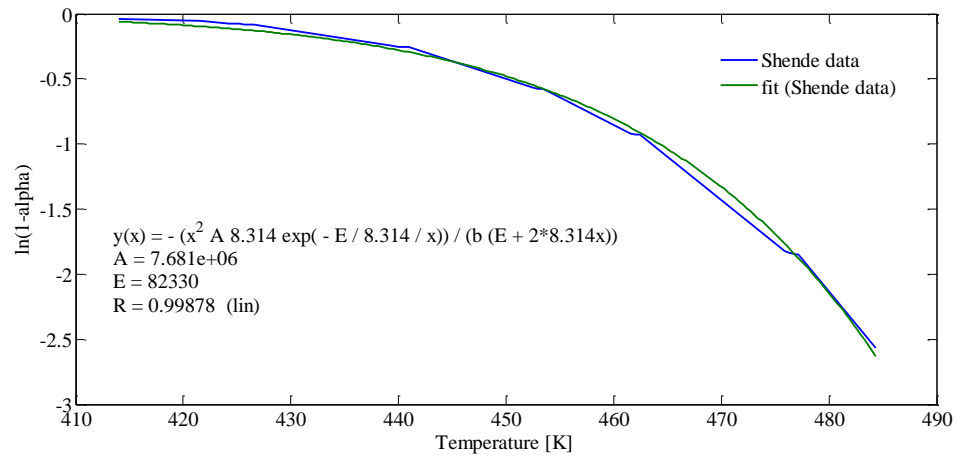
Figure 8: Fit of Shende's PVB weight loss data[1] using the integral method[3] for $\beta = 1^{\circ}C \cdot \text{min}^{-1}$ to determine kinetics parameters.

To see the weight loss for the parameters we determined using curve fitting

equation (17) must be solved. The COMSOL Multiphysics pde interface can be used easily

to solve this differential equation. The weight loss as a function of temperature is displayed

in Figure 9 for the parameters we found by curve fitting as well as the parameters[1]

published in Shende's paper using the integral method[3]. While the parameters we obtained

in our fit are relatively close to the parameters that Shende finds, clearly the difference in

parameters greatly effects the weight loss profile, as we expected. While they both describe

the rate of weight loss similarly, the difference in onset of weight loss is quite different, ~30 °C. Yet, we again attribute this to the digitization limitations, whereas experimental data will give far more accurate results.
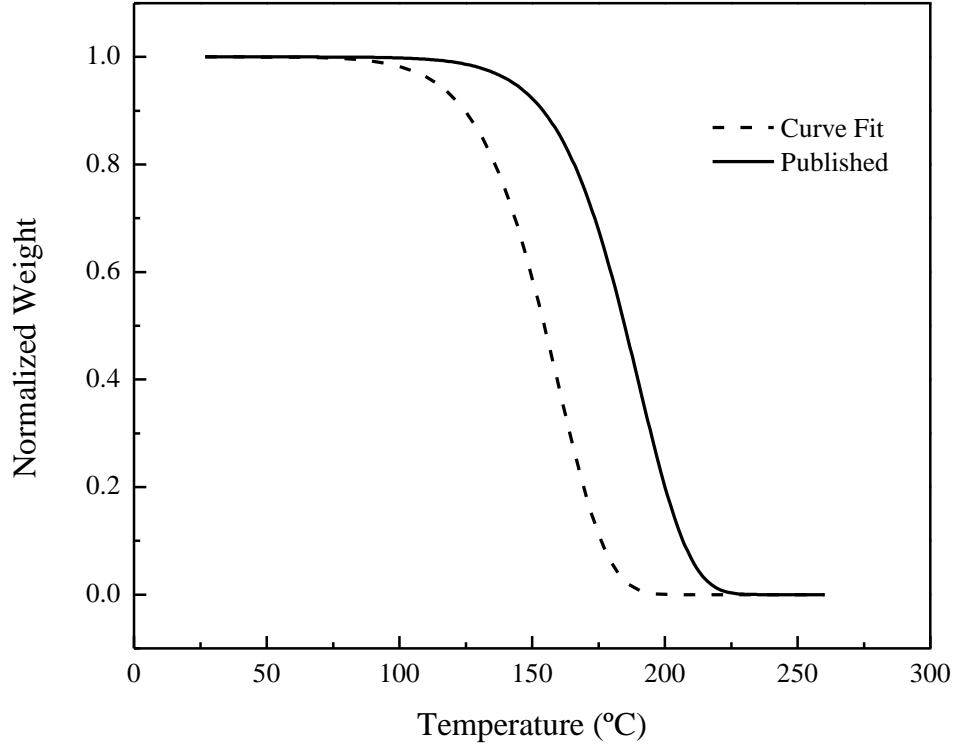
Figure 9. Weight loss using curve-fit parameters and published parameters in an Arrhenius reaction rate with $\beta = 1° C \cdot \min^{-1}$.

2.2   Creating a Numerical Model for Pressure

To develop a model that tracks the evolution of binder removal in a ceramic green body, a method of validating past work is necessary. Therefore, we proposed to develop a numerical model using COMSOL Multiphysics following the theory that Shende uses to create an analytical model for pressure, Equation (13). The published results are validated

as a benchmark to ensure that the methodology being used to solve the system numerically, Equation (10), is correct. To implement a model evaluating the internal pressure of a body, a variety of parameters are necessary as input. A majority of the parameters is based on the characterization of the specimen. The parameters necessary are presented in Table 1 and the necessary variables in Table 2 for Shende's model[1] involving the removal of binder in a PVB-BaTiO$_3$-Pt multilayer capacitor (MLC). The reaction kinetics, as described by the fitting method above, has already been determined.

COMSOL Multiphysics is a finite element analysis package that is particularly useful when coupled phenomena are involved. Multiple physics are occurring during the removal of binder, including reaction, mass transport, and heat transfer. COMSOL has the ability to process all of these physics simultaneously and simulate their combined effect. The steps taken to build the pressure ratio model, developed by Shende[1], in COMSOL is presented in the Appendix. To corroborate the accuracy of the COMSOL numerical solution to Shende's analytical expression, the following procedure was performed. Shende's pressure data were digitized and compared to the analytical expression solved for in Matlab (Figure 10). The Matlab solution was then compared with the COMSOL numerical model (Figure 11) to determine that the finite element solver was properly executing the numerical analysis.

Table 1: Parameters necessary for input in a model solving for internal pressure within a ceramic green body.   Values are from Shende's PVB-BaTiO$_3$-Pt MLC[1] with $\beta = 10°C \cdot \min^{-1}$

Name	Expression	Value	Units	Description
E		151000	J.mol^{-1}	activation energy
A		8.5 x 10^{15}	s^{-1}	pre-exponential factor
R		8.314	J.mol^{-1}K^{-1}	universal gas constant
T_init		300	K	initial furnace temperature
beta		10	°C.min^{-1}	linear heating rate
Vg0_frac		0.19		initial porosity fraction
Vb0_frac		0.31		fraction of body occupied by binder t=0
Vs0_frac		0.5		fraction of body occupied by ceramic t=0
L		0.01	m	body half-length
Vt0	(2L)^3		m^3	initial total volume of body
Vb0	Vb0_frac x Vt0			initial binder volume
M_gas		0.044	kg.mol^{-1}	average molecular weight of gas phase products
rho_b		1000	kg.m^{-3}	constant density polymer
mu		2.5 x 10^{-5}	Pa.s	viscosity of the gas
k		5		constant accounting for shape and tortuosity of pores
S		6 x 10^6	m^{-1}	surface area per unit volume of the body
P_0		1 x 10^5	Pa	initial pressure
chi		9 x 10^{-7}	m^2.s^{-1}	thermal diffusivity
Vb_stop	mod1.minop1(mod1.Vb)		m^3	the time where the local minimum Vb is negative
k_tcb		0.2	W.m^{-1}.K^{-1}	thermal conductivity binder
k_tcs	mod1.mat1.def.k11		W.m^{-1}.K^{-1}	thermal conductivity ceramic from material library
cp_b		2080	J.kg^{-1}.°C^{-1}	heat capacity of binder
cp_s	mod1.mat1.def.Cp		J.kg^{-1}.°C^{-1}	heat capacity of ceramic
cp_g		0.839	J.kg^{-1}.°C^{-1}	heat capacity of gas

Table 2: Variables necessary for input in a model solving for internal pressure within a ceramic green body.   Values are from Shende's PVB-BaTiO$_3$-Pt MLC[1] with β = 10°C·min^{-1}.

| Name	Expression	Units	Description
T_furnace	T_init + beta x t	K	furnace temperature
alpha	1-Vb/Vb0		fraction of binder reacted
Vg_frac	1-Vs0_frac-Vb_f		instantaneous volume fraction of gas
Vb	Vb_f x Vt0	m^3	instantaneous volume fraction of binder
r	A x exp(–E/R/T_furnace) x (1-alpha) x rho_b	s^{-1}	reaction rate
kappa	Vg_frac^3/(k x (1-Vg_frac)^2 x S^2)	m^2	permeability of the gas in pore space
phi_inst	Vg_frac		instantaneous porosity
p_frac	p/P_0		pressure fraction
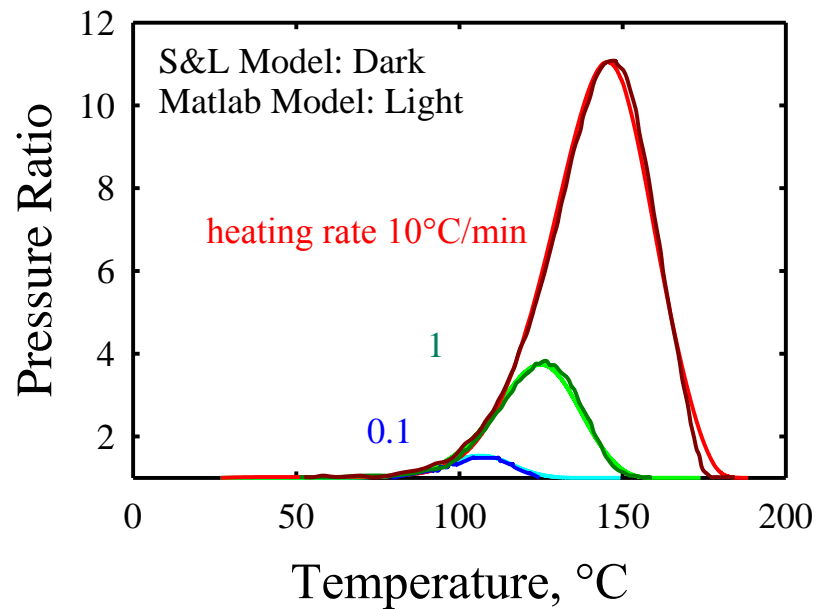
Figure 10: Digitized version of Shende's[1] analytical expression for internal pressure ratio compared to the expression as solved for in Matlab.
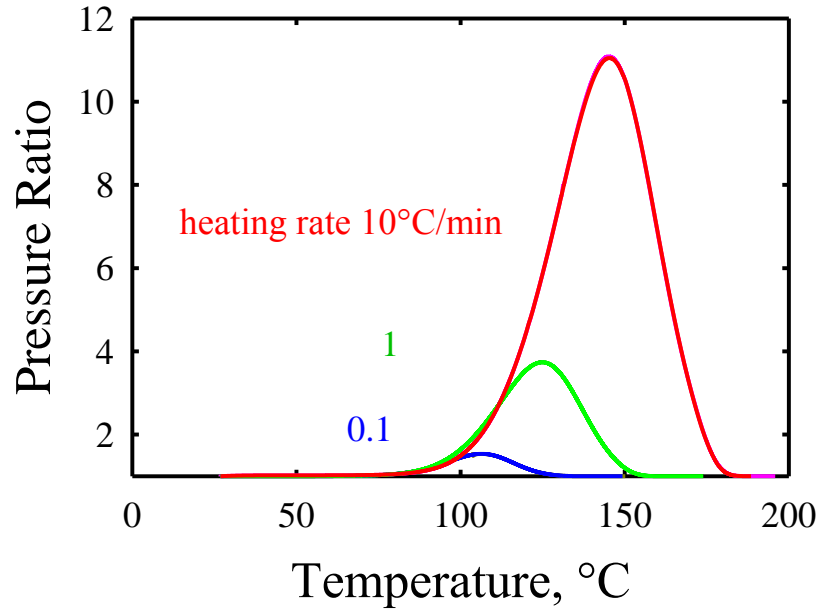
Figure 11: Shende's[1] internal pressure ratio expression solved for in Matlab compared to the numerical solution for pressure ratio solved numerically by COMSOL.

The comparison of Shende's analytical model for pressure ratio with a COMSOL model solving for pressure using the same assumptions and parameters (no internal heat transfer, pressure is at the centerline of the body, homogenous removal, and pseudo-steady state) in Figure 10 and Figure 11 verify the numerical solving capabilities of COMSOL.

While the analytical model developed by Shende is useful for tracking internal pressure along the centerline of the body, it lacks aspects that could affect the model accuracy and is missing functions in which a user of the model may be interested in. The assumptions made, which as stated previously are: $\frac{\partial T}{\partial x} = 0$, $\frac{\partial V_b}{\partial x} = 0$, and $\frac{\partial}{\partial t}(V_g \bar{\rho}) = 0$, may not have a large impact on the particular combination of materials being studied in Shende's paper, but could have a more significant effect on a different set of materials and/or different set of parameters and geometries. For these reasons, the use of a numerical

solver such as COMSOL Multiphysics is very beneficial as it is not limited to a single system. The coupling of all the possible effects during debinding is a very useful tool.

The ability to track the internal pressure along the centerline of the body is the most practical scenario for open porosity as the pressure will be greatest there. On the contrary, systems of interest that are not open porosity, such as injection molded parts, will likely have maximum internal pressure along the interface. Therefore, depending on the context, the pressure at other geometrical locations may be of interest, as well as studying pieces that are of more complex geometry than the cube studied. Lastly, a more accurate method of fitting the weight loss data is desired to represent the true nature of the material's thermal degradation sequence.

2.3   Multiple Volatile Species Created During Thermal Degradation

The thermal degradation of polymer may occur in stages where different units of the polymer detach from the main chain at different temperatures. Multiple methods exist to model this process. The species could break off in series or in parallel, among other possibilities. A parallel volatile reaction implies that once the first polymer species begins volatizing and transporting out of the body, the second species may begin reacting but is independent of the first species. In a series reaction, the first reaction occurs creating an intermediate solid and a volatile species. The intermediate solid has a unique reaction temperature, which creates a second intermediate solid and volatile species. This process continues until only a gas or inert solid remain. With the series reaction, the rate at which an intermediate solid reacts is dependent on how much intermediate solid the prior reaction has created.

The reaction model ultimately used to solve for internal pressure is based on the best fit to the weight loss data. While the physics of one scheme may seem more reasonable in a given reaction, some variables may arise in the reactions for which are difficult to account. This could lead to a more physically unexpected reaction mechanism being a better fit to the weight loss data.

Another variable in determining the best fit to weight loss data is the reaction order. For simplicity, equation (4) is a first-order reaction so that Lee and Beck's integral method[3] can be used to fit weight loss data, but the order of reaction can be changed depending on how it fits best.

An example of how a reaction might degrade in parallel is presented in Figure 12. In this thermal reaction, as the molecule heats up it will undergo random scission whereby pieces of the long-chain are cleaved at their respective temperatures and may become volatile matter.
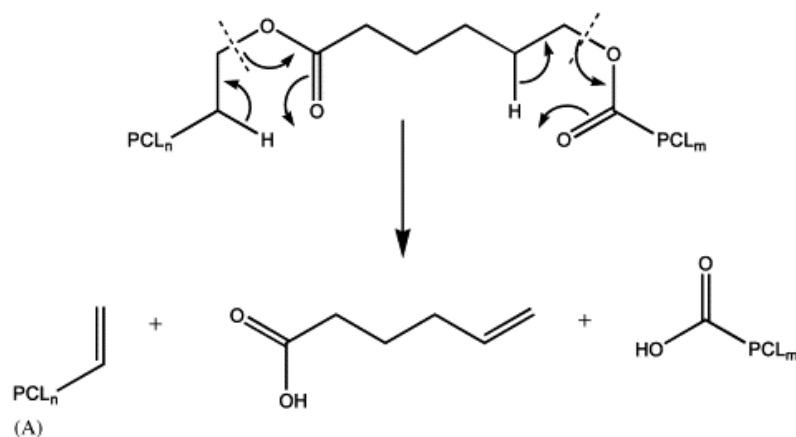

Figure 12: Random scission reaction of poly(ε-caprolactone)[4] portraying a degradation reaction in parallel.

In this scenario, the reaction of the individual volatile species can occur at any moment; their reaction is not dependent on the progress of other species' reactions.

The case of a series reaction is presented in Figure 13. The initial reaction that occurs creates two products, one of which may be volatile matter. The second, non-volatile product then undergoes its own reaction at a subsequent temperature and produces gaseous volatile species, more species that will take on further reaction, or an inert species. The degradation will continue until only gaseous species and/or inert species exist. During this reaction, each species reaction rate, since it is a function of how much material remains in equation (17), is highly dependent on the progress of the preceding reaction.
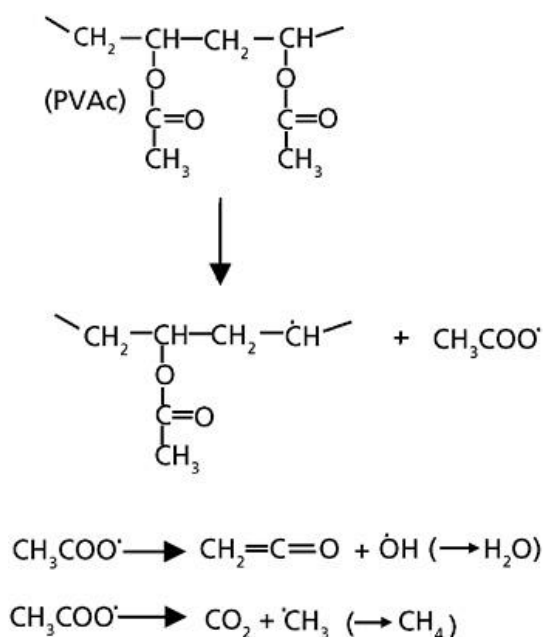

Figure 13: Free radical reaction mechanism[5] for degradation in poly vinyl acetate (PVAC) portraying a series degradation reaction.

3. Computational Model

3.1 Reaction Scenarios Modeled in COMSOL

A method for determining what mechanisms are occurring during degradation is to model the scenarios and see what agrees best with the weight loss data from TGA experiments. Since a model for pressure is dependent on the reaction rate, as long as the modeled reaction rate is representative of the data, the physics behind the model is more of a curve fitting tool than a description of the physical process.
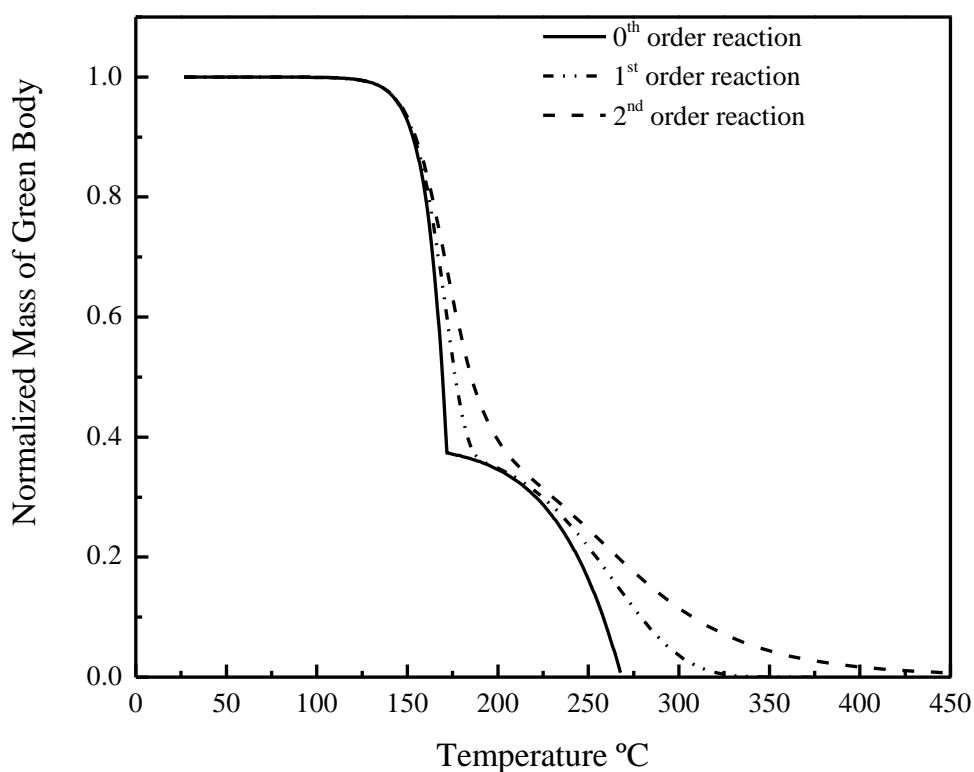

Figure 14: Weight loss solved by COMSOL for two species degrading in parallel for different orders of reaction. Heating rate is 10 °C·min^{-1} with $A_1 = 8.5 \times 10^{15}$ s^{-1}, $A_2 = 4.5 \times 10^3$ s^{-1}, $E_1 = 151$ kJ·mol^{-1}, and $E_2 = 61.9$ kJ·mol^{-1}.

The order of a reaction is determined by finding the best fit to experimental data. In fact, a guess-and-check method is often used to find the most accurate reaction order.[15] The effect the reaction order has on the weight loss profile for a two species degradation model is presented in Figure 14. It can be seen that the 0th order reaction creates a sharp break between the reaction rates of the two species, whereas the higher order rates have a smoother transition. This occurs when there is no dependence on the amount of material present.

Another variable that affects the weight loss profile of a green body is the heating rate. Figure 15 exhibits how the weight loss curve is affected by the heating rate given the same kinetics parameters for each heating rate. It is clear that the profile loses its shape as the heating rate is decreased, whereas the shape becomes more pronounced as the heating rate is increased. Through the use of COMSOL, the ability to notice such trends is a useful tool in determining how to best fit experimental data.
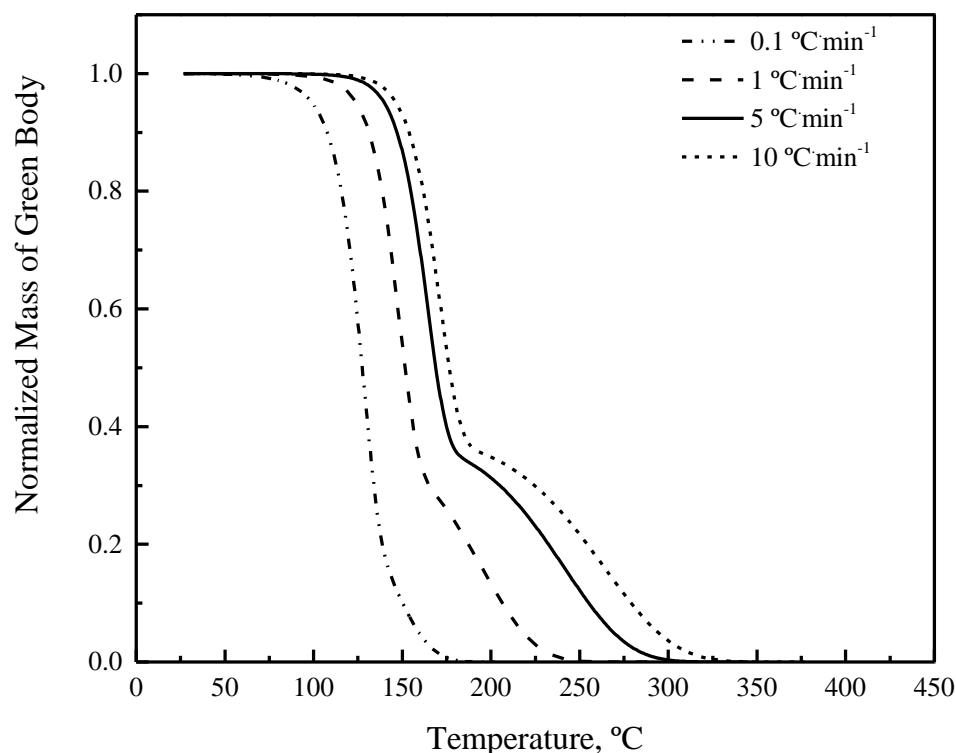
Figure 15: Weight loss solved by COMSOL for two species degrading in parallel for different heating rates in a 1st order reaction with the same kinetics parameters as Figure 14.

The amount of each volatile species that degrades will affect the weight loss profile of the body. While it may be difficult to experimentally determine the quantity of each species, the amount of each species can easily by modified in COMSOL. The effect that two different species degrading has on the green body is presented in Figure 16, where the weights are normalized to the initial binder mass. Figure 17 displays the corresponding reaction rates to the species in Figure 16. By changing the reaction rates, and in effect the weight loss profile of each individual species, it is apparent how the weight loss profile of

the green body is changed. This is yet another tool that COMSOL provides to find the best fit to experimental data.

Having such a powerful numerical solver is extremely useful when the physical behaviors of a process, particularly coupled physics, are not accurately known. Having the ability to easily evaluate many values at once given a range of parameters allows the user to find the best match to the physics by comparing to the results of experimental data.
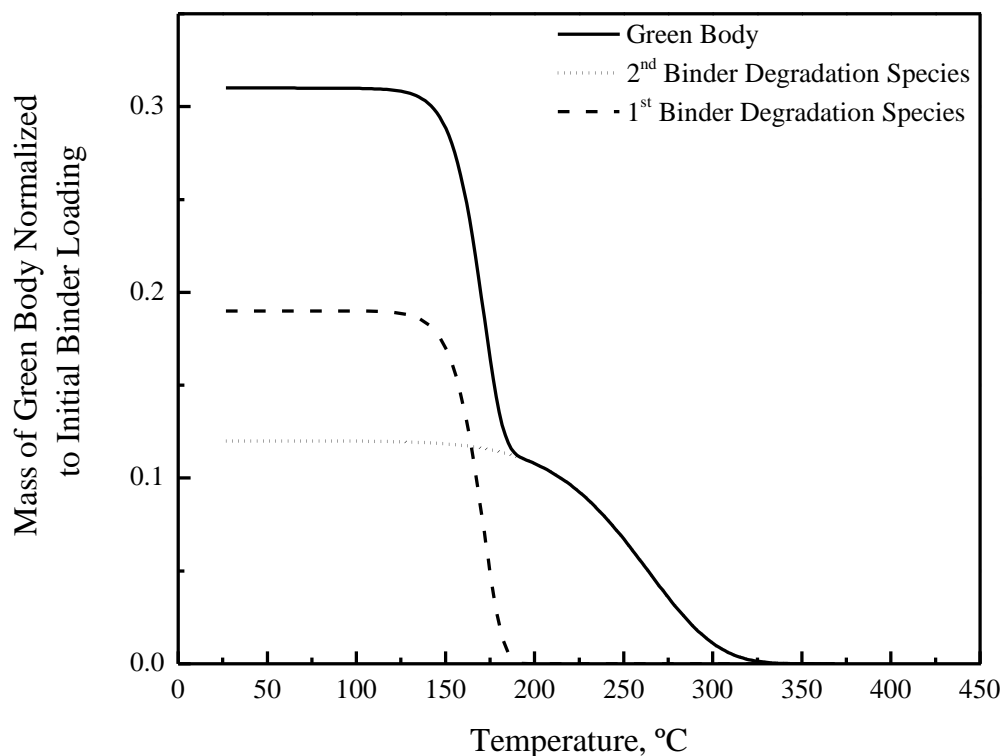

Figure 16: Weight loss of degradation species and green body solved by COMSOL for two species degrading in parallel. Reaction is 1st order and heating rate is 10 °C·min^{-1} with the same kinetics parameters as Figure 14.
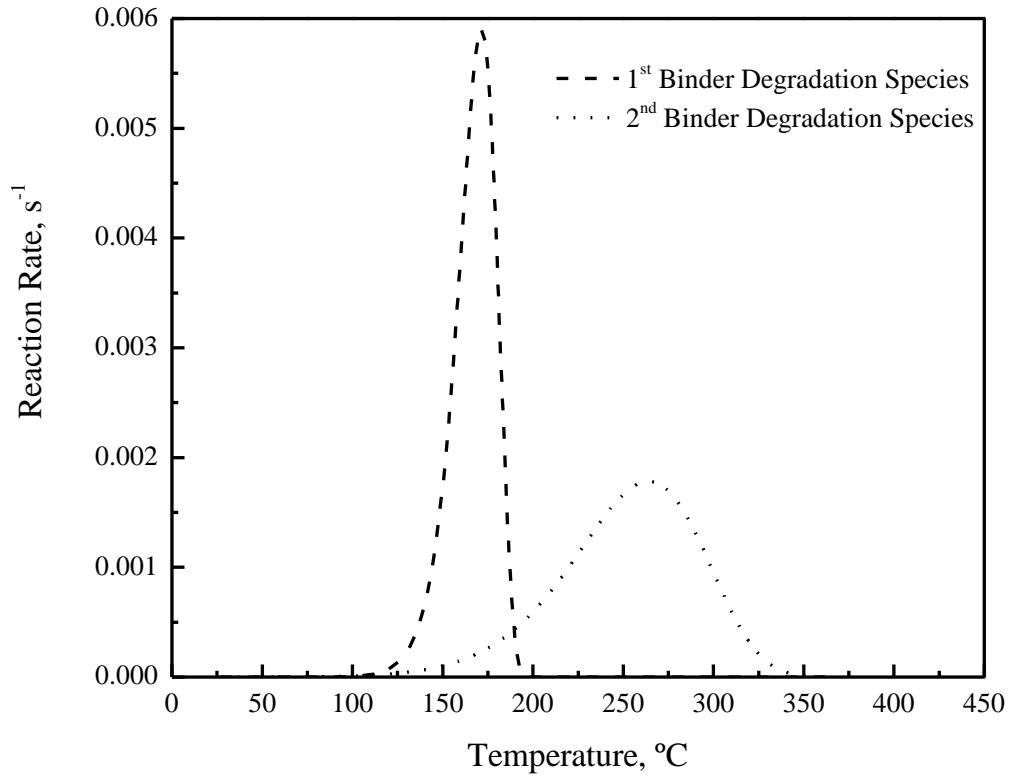
Figure 17: Reaction rates solved by COMSOL for two species degrading in parallel for a 1st order reaction. Heating rate is 10 ℃·min^{-1} with the same kinetics parameters as Figure 14.

Once an acceptable fit is determined, the kinetics parameters calculated from that fit can be input into the model that determines internal pressure buildup according to Equation (10). Assuming that the green body parameters and variables are known from Table 1 and Table 2, the pressure can be modeled as displayed in the plot in Figure 18. Considering the pressure is numerically calculated by solving a partial differential equation, it is not unusual for COMSOL to encounter errors while evaluating for pressure. When such a glitch or runoff variable is noticed, the solver settings must be manipulated. Some solver changes in particular that proved useful in computation are creating a smaller

or larger time step, changing the size of the mesh, and changing the solver time step from free to strict.
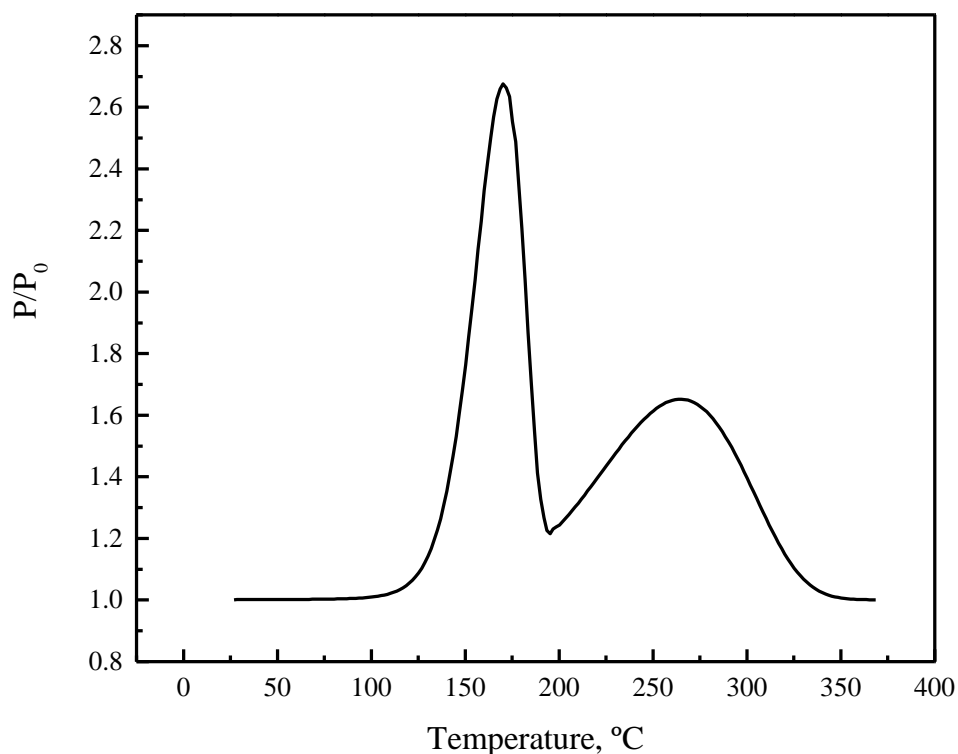
Figure 18: Internal pressure ratio along the centerline of the body solved by COMSOL for two species degrading in parallel for a 1st order reaction. Heating rate is 10 °C·min^{-1} with $A_1 = 8.5 \times 10^{15}$ s^{-1}, $A_2 = 4.5 \times 10^3$ s^{-1}, $E_1 = 151$ kJ·mol^{-1}, and $E_2 = 61.9$ kJ·mol^{-1}.

While Shende evaluated the pressure along the centerline of a green body, COMSOL tracks the pressure (among the many other variables it solves for) over the entire geometry. Shende's model also includes the assumption that the temperature is uniform throughout the body. While this assumption is valid for small samples and samples that are very thin compared to its other dimensions, this assumption would likely fail with an

increase in size or dimensions of the green body. The difference in the weight loss profile

for a body with and without heat transfer within the body is presented in Figure 19. In this

model, the only internal heat transfer considered is conduction due to the ceramic material

(in this case BaTiO$_2$). The heat transfer characteristics of the binder could be included as

well by adding a second domain.
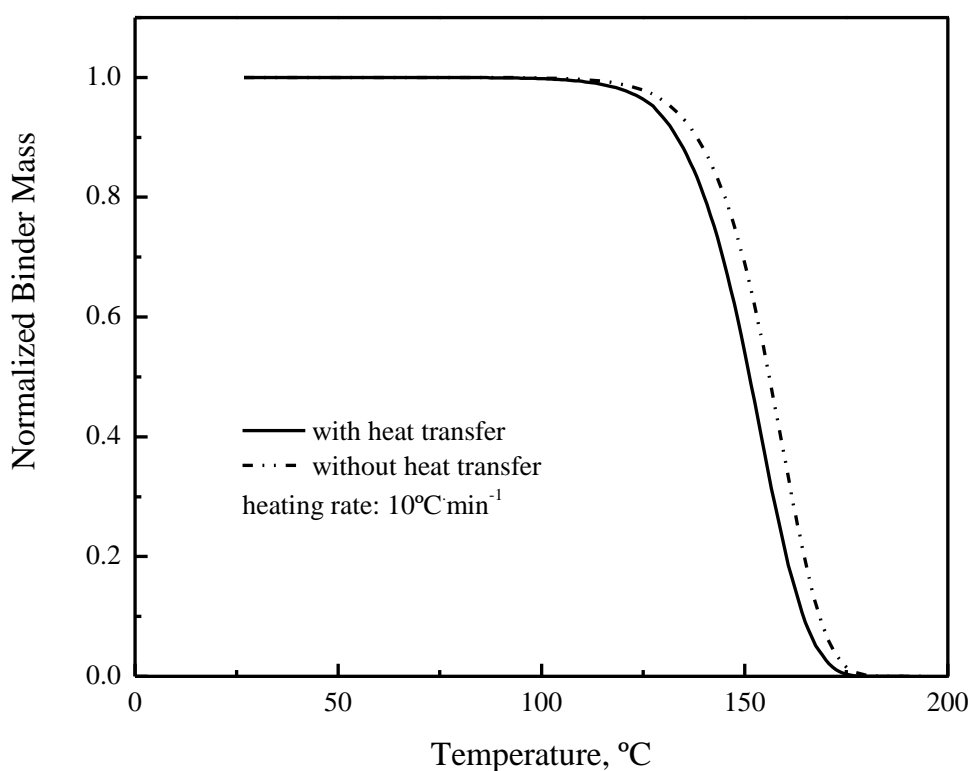
Figure 19: Weight loss solved by COMSOL for two species degrading in parallel. One model includes internal temperature gradients while the other does not. Reaction rate is 1st order and heating rate is 10 °C$\cdot$min^{-1} with $A_1 = 8.5 \times 10^{15}$ s^{-1}, $A_2 = 4.5 \times 10^3$ s^{-1}, $E_1 = 151$ kJ$\cdot$mol^{-1}, and $E_2 = 61.9$ kJ$\cdot$mol^{-1}.

COMSOL's ability to evaluate variables along the entire geometry is displayed in

Figure 19. The different colors represent various time steps during the heating sequence

and the instantaneous temperature at the given spatial location. While the internal pressure during a heating sequence is likely to be greatest at the center of a symmetric body, a body with unusual geometry will not exhibit the same behavior. It is useful to evaluate the pressure as well as any other model variable anywhere in the geometry of the body.

For simplicity, the model created is a one dimensional model. It is possible to develop a multi-dimensional model as well in COMSOL, which has the capability of solving geometries more complex than a disk or a cube.
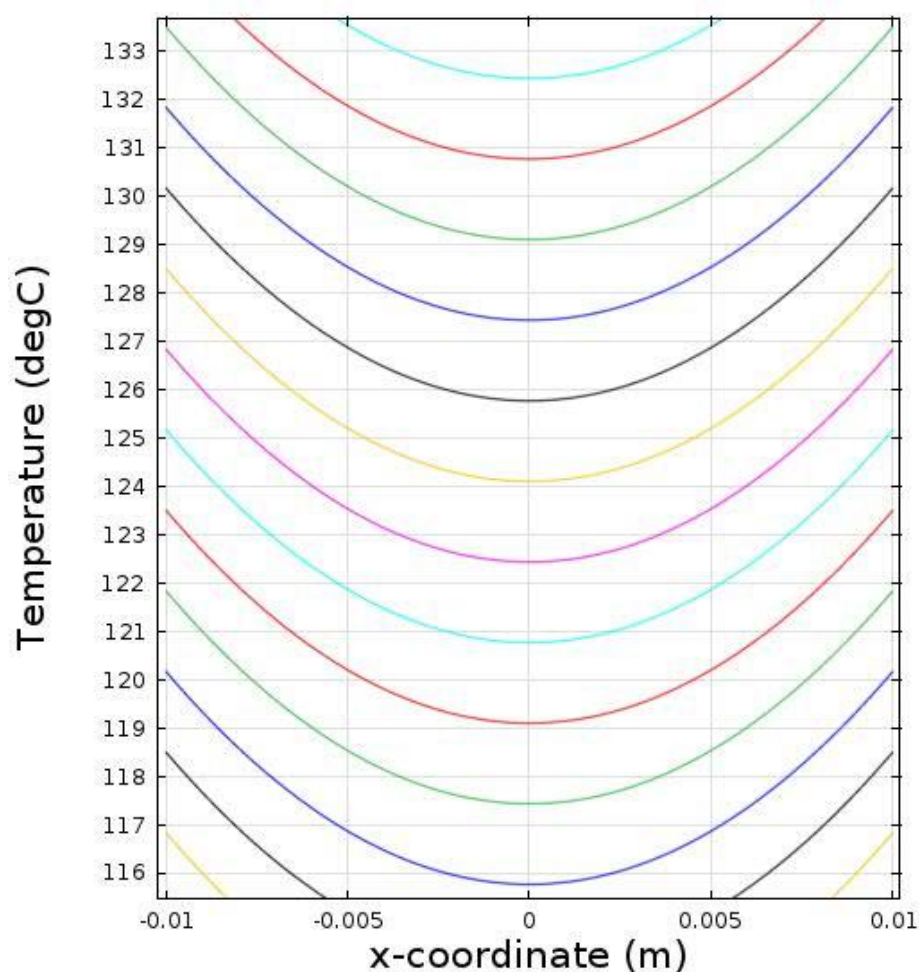

Figure 20: Temperature profile for by COMSOL for two species degrading in parallel for a range of times during heating sequence. Model includes temperature gradients. Heating rate is 10 ℃·min^{-1} with the same kinetics parameters as Figure 19.

It is a valuable exercise to examine how varying certain parameters affect the weight loss profile of a green body that degrades with series reactions. Figure 2 presents reactions in series in 1st and 2nd order. The reactions are based on those formulated by Dirion *et. al*[12] for three species and two reactions, similar to the reaction in Figure 5.

When analyzing the effects of reaction order on the weight loss profile, a 0th order reaction is not presented. In the case of a reaction in series, since the creation of each
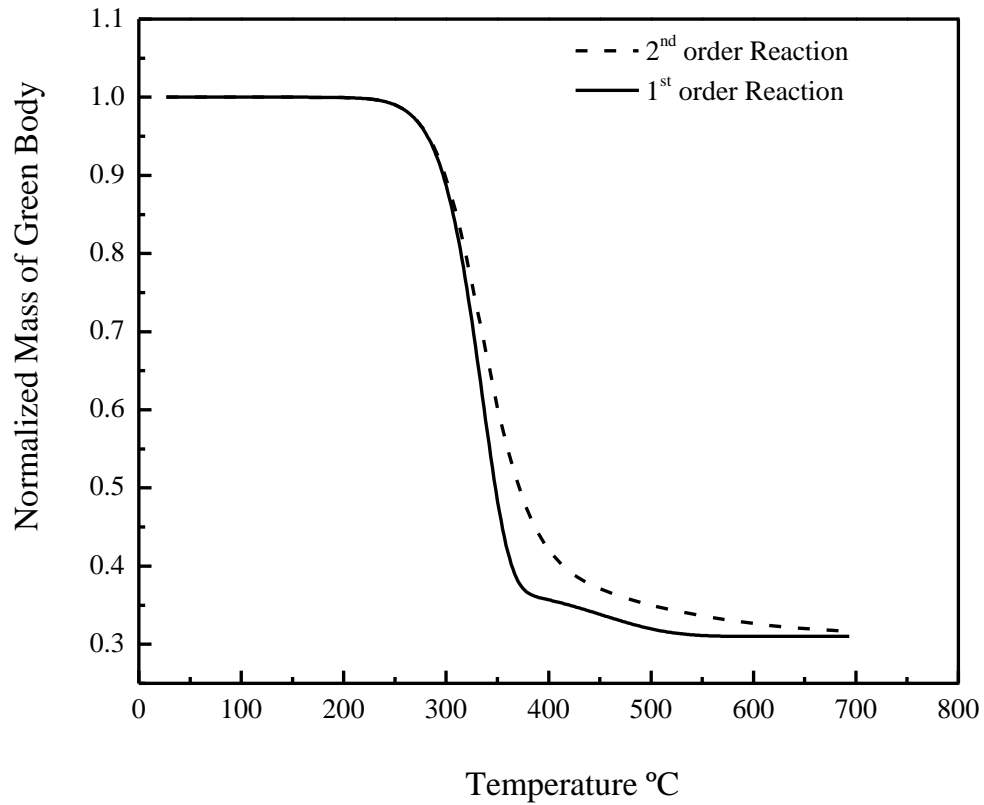

Figure 21: Weight loss solved by COMSOL for three species, two reactions which are in series, for different orders of reaction. Heating rate is $10\ °C·min^{-1}$ with $a = 0.37$, $b = 0.31$, $A_1 = 7.8267×10^7\ s^{-1}$, $A_2 = 367.11\ s^{-1}$, $E_1 = 117.5\ kJ·mol^{-1}$, and $E_2 = 65.7\ kJ·mol^{-1}$.

species is dependent on the progress of its preceding reaction, if no material dependence exists in the reaction equation, (17), the intermediate reaction will never occur. The weight loss in Figure 21 does not reach zero because the char that is formed in the pores is inert under a nitrogen atmosphere and its reaction is therefore complete.
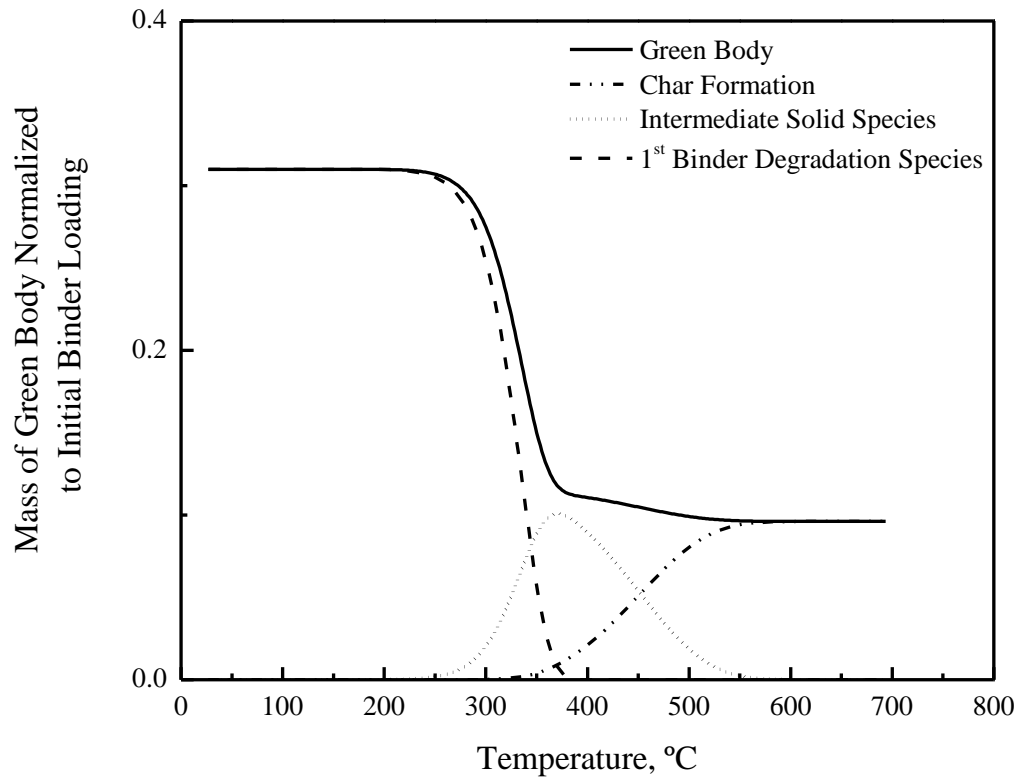
Figure 22: Weight loss of each degradation species and green body solved by COMSOL for three species, two reactions which are in series. Heating rate is 10 °C·min^{-1}, reaction is 1st order, with the same kinetics parameters as Figure 21.

Figure 22 presents how the weight loss of individual degradation species affects the green body's weight loss. It is validating to notice how the rate of the green body's weight loss is slightly less than the 1st volatile species' weight loss until the intermediate solid

species reaches its inflection point. At this point, ~390 ºC, the green body weight loss shallows out. Also important to notice is the meeting of the char mass and green body mass, signifying the completion of the reaction at ~560 ºC.

The respective reaction rates from the three species presented in Figure 22 are displayed in Figure 23. A negative reaction rate arises from the full binder degrading and creating an intermediate binder species and a gaseous species. The intermediate species has positive and negative reaction rates due to its creation from the first reaction and then its degradation during the second reaction. It is a function of two reactions and their proportionality constants, equation (5). The char has a positive reaction rate because it is a product of the second reaction and the char product is inert so it does not undergo a further reaction.
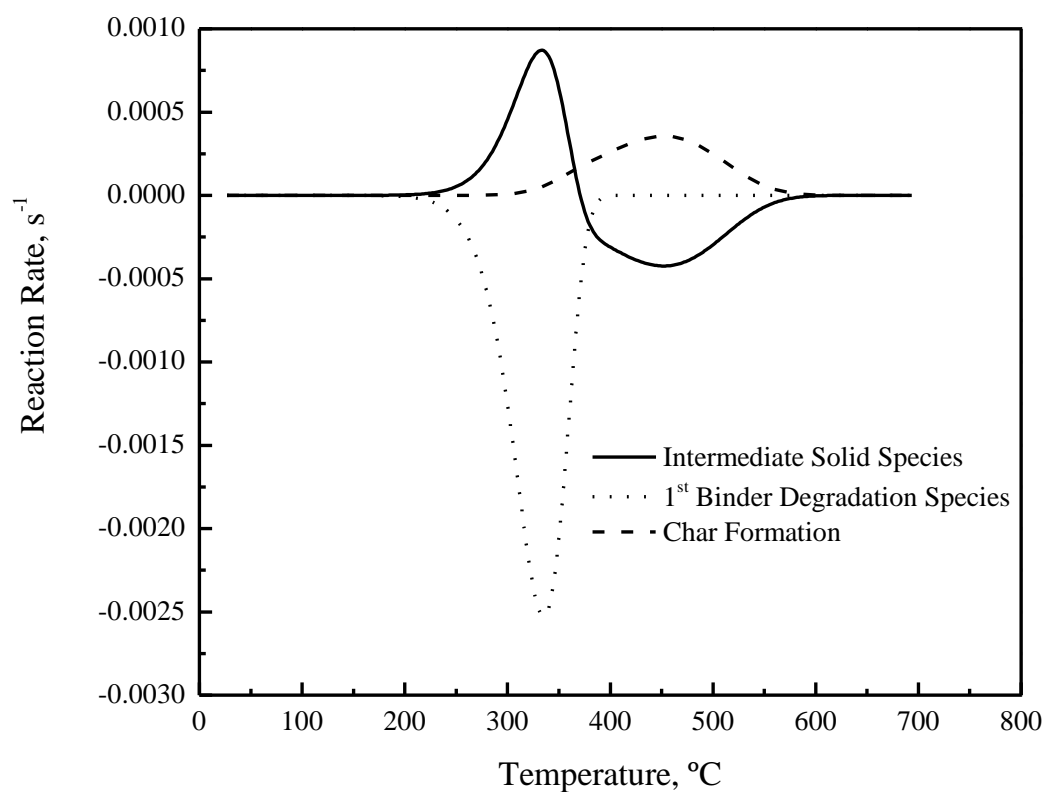
Figure 23: Reaction rates solved by COMSOL for three species, two reactions which are in series. Heating rate is 10 ℃·min^{-1}, reaction is 1st order, with the same kinetics parameters as Figure 21.

4. Experimental Work

A common way of validating any phenomenological model is to compare with experimental data. Two samples were obtained for experimentation. Poly vinyl alcohol (PVA) in an aqueous solution was obtained from Saint-Gobain that was 21% weight active ingredient. A pressed sample of Titanium Oxide (TiO$_2$) was obtained from a Laboratory Researcher in the department, Asad Mughal. The sample was prepared using Pfaltz & Bauer TiO$_2$ Anatase 99%, Lot 106, T13399. Fourteen grams of the powder were mixed

with 2mL of aqueous PVA solution (CAS 9002-89-5 F.W. 44.05), freeze dried, and pressed at 79MPa. Both the PVA alone and TiO_2+PVA samples were run in a TA Instruments TGA Q5000 during the same testing sequence. They were allowed to equilibrate at 50 ℃ and held there isothermally for 5 minutes then a 5 ℃•min^{-1} temperature ramp was employed to 1000 ℃. The raw data from the PVA and TiO_2+PVA TGA experiments are presented in Figure 24 and Figure 25, respectively.
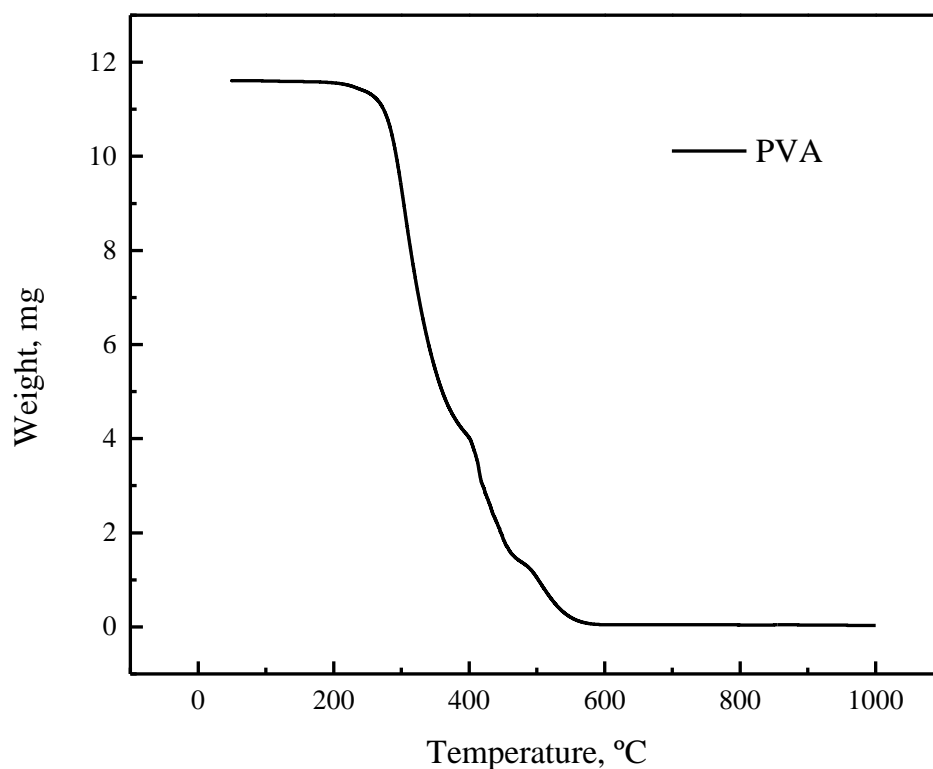
Figure 24: Raw TGA data for PVA alone at a heating rate of 5 ℃•min^{-1}. The aqueous solution (21% by wt. PVA) sample was dehydrated in an oven at 110 ℃ overnight.
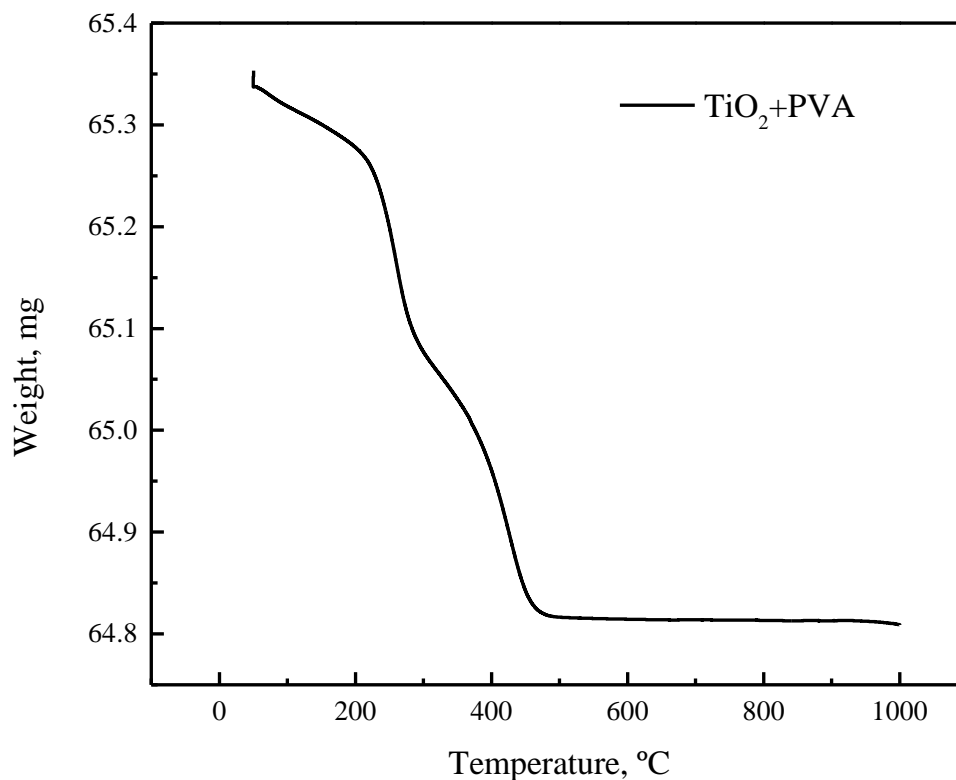
Figure 25: Raw TGA data for TiO_2+PVA at a heating rate of 5 °C·min^{-1}. The sample was freeze dried after pressing.

The weight loss curves for the PVA alone and the ceramic and binder system are shown in Figure 26. The weight loss is normalized to the initial sample weight. Some interesting features exist in the data, with the foremost being the amount of mismatch between the two compositions. Weight loss in the ceramic system begins immediately at 330 K while the PVA does not begin to lose weight until 600 K. While the PVA alone sample was dehydrated overnight to get rid of water content, the TiO_2 was not dehydrated and therefore the early weight loss could be assumed to be water.

Since the boiling point of water is 373 K, that water loss would not occur until 80 seconds after the temperature ramp begins due to boiling. Yet, evaporation of the water does occur at a temperature less than the boiling point of water, so the first weight loss can be identified as water. The PVA does not degrade in the TiO_2 until the PVA alone degrades. Therefore, the second weight loss slope of the ceramic system is not binder material. The third weight loss region in the TiO_2 likely is the PVA transporting out of the body in gaseous form. Its degradation occurs at a temperature slightly, ~25 K, greater than the PVA alone (600 K) due to the time it takes transport out of the body.

A final possibility of why the ceramic and binder system behaves different from the PVA alone is due to the sample preparation. It could be the case that the TiO_2+PVA sample obtained had already undergone binder removal. Therefore, a PVA weight loss would not be expected. Yet, the same TiO_2+PVA sample that was known to have undergone binder removal was obtained and run in the TGA at 5 °C·min^{-1}. It was confirmed that the original sample did in fact have binder present in the green body. The weight loss curve of the sample having undergone binder removal showed negligible weight loss whereas the initial sample tested had distinct weight loss.
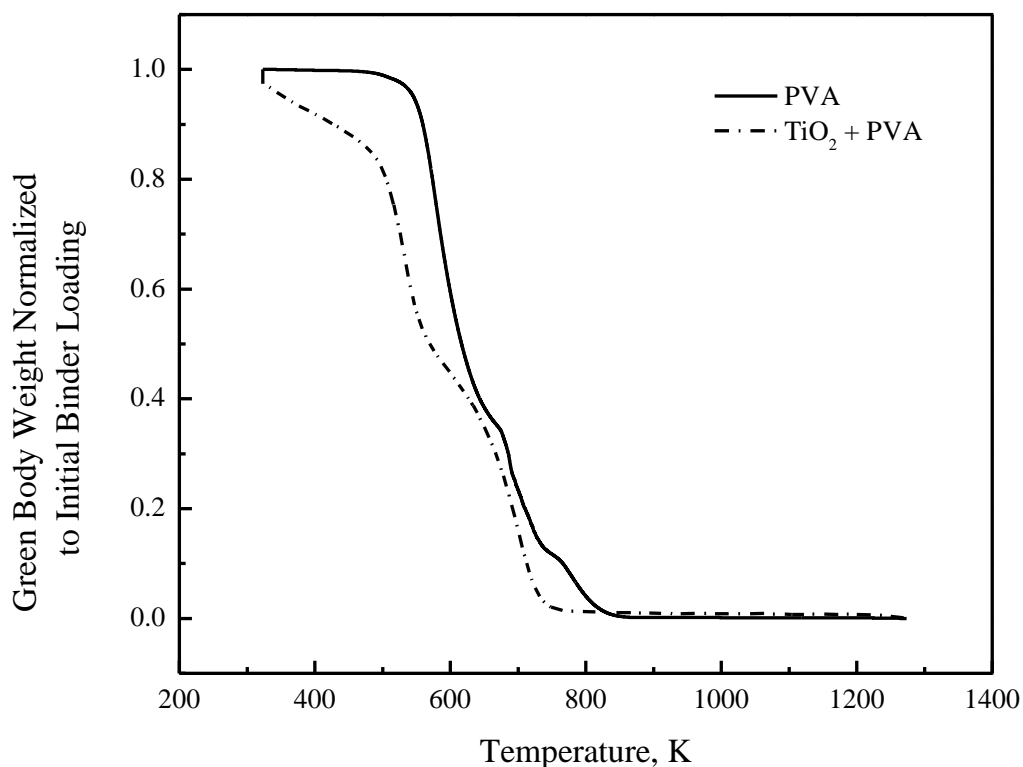
Figure 26: TGA weight loss data are for PVA alone. Data is normalized to initial weight compared with TiO_2+PVA weight loss normalized to initial binder weight at a heating rate of 5 °C·min^{-1}.

It is difficult to determine from this particular weight loss curve how many different species are being transported out of the body and how many separate reactions are occurring. Therefore, the simplest case is to fit to the data to analyze its effect in a model. A first-order, single species reaction is fit to the PVA alone and presented in Figure 27. The kinetics parameters for the PVA alone were determined to be $A = 41.59$ s^{-1} and $E = 54613$ J·mol^{-1}.
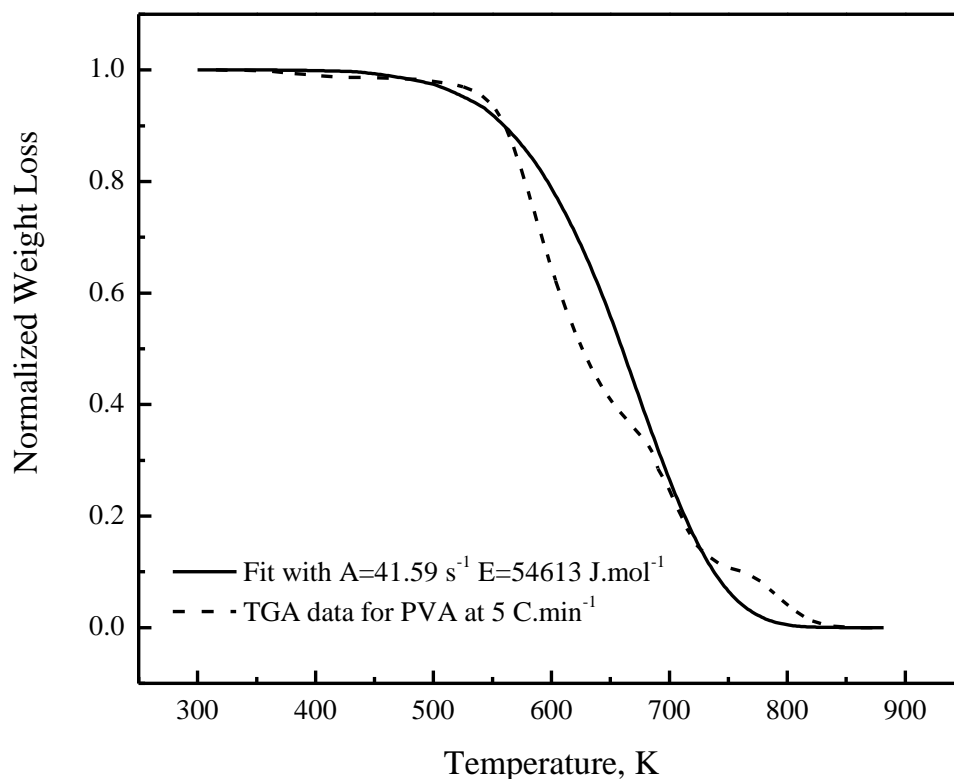
Figure 27: TGA weight loss data for PVA alone normalized to initial weight. A single species, 1st order reaction was fit using the parameters $A = 41.59$ s^{-1} and $E = 54.6$ kJ·mol^{-1}. Heating rate is 5 °C·min^{-1}.

While the kinetics parameters determined from this fit do not describe the shape of the first and last portions of the weight loss data, they do accurately describe the onset and termination of the weight loss sequence.

To determine the internal pressure buildup in the TiO_2 given this single species degradation profile of the PVA binder, certain parameters must be determined as model input. The volumetric distribution of the sample must be determined. The volume of the bulk material is calculated using a radius of 25.12 mm and thickness of 3.6mm to be 1.78 cm^3. The mass of the pellet is 3.531 g so using a density of 4.23 g·cm^{-3} for TiO_2, the

particle volume of TiO_2 is 0.835 cm^3. Since the sample has 2.06 mL of aqueous solution that has 5% by volume PVA, we know the particle volume of the PVA to be 0.103 cm^3 in the batch that was processed. Multiplying the mass fraction of the pellet to the batch by the binder volume tells the volume of binder in the pellet, or 0.026 cm^3. Therefore, the sample has a porosity of 0.512 and the following volume fraction distributions:

$$\text{Volumetric bulk density, } V_T = \pi \left(\frac{25.12 \text{cm}}{2} \right)^2 0.36 \text{cm} = 1.764 \text{cm}^3$$

$$\text{PVA Particle Volume, } V_{PVA} = 2.06 \text{cm}^3 (0.05) \frac{3.531g}{14g} = 0.026 \text{cm}^3$$

$$\text{TiO}_2 \text{ Particle Volume, } V_{TiO_2} = \frac{3.531g}{4.23 \frac{g}{\text{cm}}} = 0.835 \text{cm}^3$$

$$\text{Porosity, } V_g = 1 - \frac{V_{PVA} + V_{TiO_2}}{V_T}$$

$$V_b = 0.015 \quad V_s = 0.473 \quad V_g = 0.512$$

Figure 28: Calculations to determine the volume fractions of binder content, porosity, and ceramic for the TiO_2+PVA system.

These volume fraction distributions, along with the kinetics parameters found during the fit in Figure 27, can be input into the COMSOL model for internal pressure, shown in Figure 29. This plot shows the buildup of pressure as temperature is ramped and weight loss begins. The maximum pressure occurs at 638 K, where the normalized weight is 0.42 and the pressure ratio is 1.38.

This is the most basic scenario that can be modeled. A single species degradation and first order fit was applied to the TGA weight loss data in Figure 27. The parameters
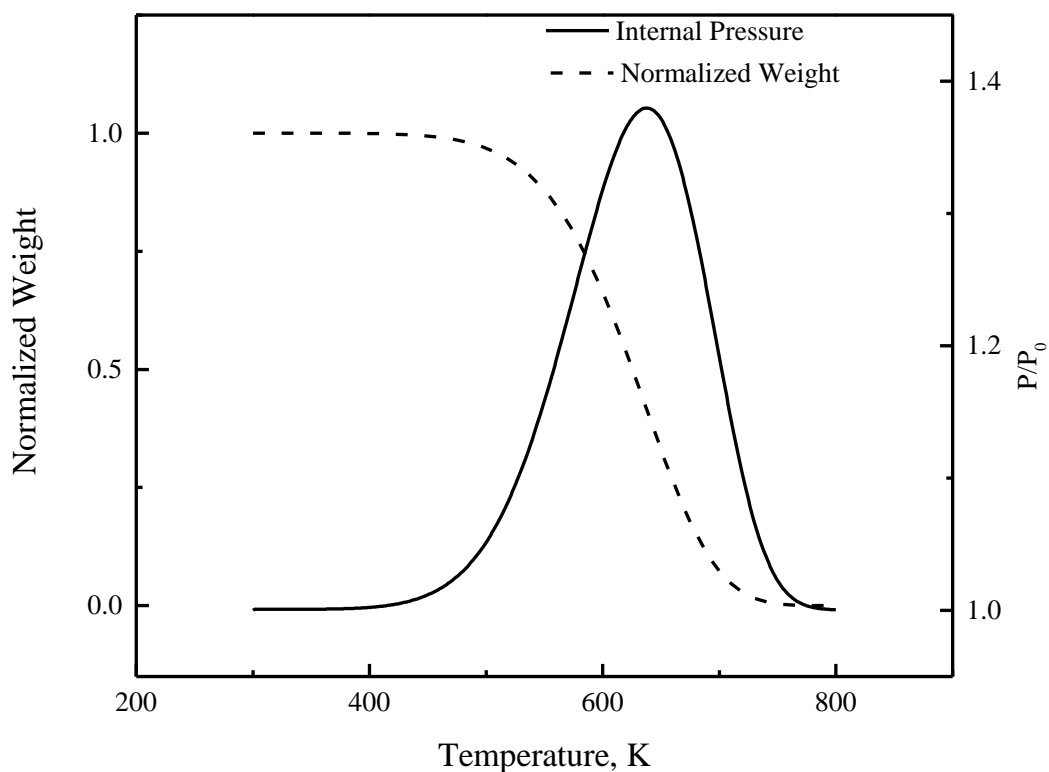
Figure 29: Model for a first order, single species degradation reaction of TiO_2+PVA at a heating rate of 5 ℃·min^{-1} showing the weight loss and internal pressure ratio along the centerline of the body.

determined from the fit were input into a COMSOL model that solved for pressure along the centerline of the cylindrical sample.

Various steps can be added or modified, to the user's liking, to increase the accuracy of the model results. The TGA data could be fit according to a degradation reaction that includes more than a single species of volatile material. The species can be fit by a reaction in parallel or in series. A reaction order can be chosen other than first order.

While the addition of more species requires a more advanced fitting technique, a framework has be laid out that assists in applying the kinetics parameters of best fit to a model that tracks the internal pressure evolution of a sample. The need for more advanced fitting arises for a few reasons. When using a reaction in series, the fit must include an extra parameter per degradation species for the stoichiometric coefficient. When fitting multiple species in parallel, the fit requires a modified or new formulation of the integral method, since Lee and Beck's formulation[3] is only valid for a single species first order reaction.

5. Discussion and Conclusions

A model has been presented that can track the internal pressure of a green body as it is subjected to a heating sequence for the purpose of binder removal. The model is solved numerically and uses the reaction and transport parameters of the green body as input. The reaction parameters are established by fitting to weight loss data, typically obtained through thermal analysis. It is evident that fitting to weight loss behavior is the limiting step in modeling the pressure. Fitting to simple systems is a comprehensive task to find kinetic parameters that satisfy a range of heating environments. To formally fit to weight loss behavior of more complex systems is therefore a tedious, time-consuming task.

We conclude that modeling systems that produce more than two volatile degradation species becomes a fitting exercise. While fitting to this data can provide the desired results, it does not establish the solution that was sought when beginning this project. Rather, simple systems that include one or two volatile degradation species can be modeled in a way that is telling of the physics occurring during thermal reaction. A set

of kinetics parameters can describe the behavior of such a system, which was a goal of this work.

The experimental data obtained during this work is somewhat inconclusive. A goal of this work was to demonstrate the modeling capabilities developed in COMSOL Multiphysics to track the evolution of internal pressure in a ceramic green body during binder removal. Therefore, the experimental work was more of a guideline to portray how the model could be employed and tested moving forward.

6.   Future Work

A well-established framework has been presented that paves the way for individuals interested in analyzing internal pressure during the binder removal sequence in ceramic compacts. Now that various parameters affecting the weight loss behavior have been described it is up to the modeler to fit weight loss data as needed for specific samples.

Developing more advanced formulas to fit weight loss data would be valuable. Since Lee and Beck's integral method breaks down beyond a single species or a reaction order other than one, it is necessary to find methods to fit weight loss data in more complex scenarios. This can possibly be done with a differential method of solving the reaction rate expression.

It would also be useful to determine how reaction order affects the weight loss. An understanding of what circumstances require a particular order or reaction would make fitting to weight loss much easier.

A physics interface that could be added to the model is a chemical reaction interface. It would be useful to know the exact species that degrade during a thermal

reaction. By allowing for input of the molecular structure of the polymer(s) (and the ceramic powder to account for catalytic effects), a function could be allotted for determining the thermal degradation of the polymer and the associated molecular weights, gas viscosity, *etc.*, of the volatile species created. This would provide key, accurate input for the continuity equation solving for pressure. Such input would prove more valuable and less time consuming than the current method of guess and check to find the best fit.

To test the accuracy of the pressure model in practice, the fracture strength of the green body being investigated should be determined. The optimal heating sequence for binder removal could be determined using the pressure model based on the fracture strength. This heating sequence could then be tested to determine the accuracy of the model results.

Finally, much work remains for evaluating the model. The model is sure to break down under certain circumstances, as does any numerical model, and it is important to find those limits. Since only one experimental sample was evaluated, many simple systems exist that can be tested as well as much more complicated systems.

Appendix

Building the Shende[1] pressure model in COMSOL 4.3

1. Select 1-D Dimension Space
2. Add Coefficient Form PDE and Darcy's Law physics (Add Heat Transfer in Solids if desired)
3. Select Time-Dependent
   a. Create a Parameters node under Global Definitions
      i. Input parameters from Table 1
4. Create a Variables node under Model 1 > Definitions
   a. Input the variables from Table 2
5. Create a line (interval) under Geometry 1 with Left endpoint −L and Right endpoint L
6. Create a point under Geometry 1 at 0
7. Create a Minimum Model Coupling under Model 1 > Definitions
   a. Select all domains
8. Solving for the mass fraction of binder under Coefficient Form PDE
   a. Coefficient Form PDE (c)
      i. Select all domains
      ii. Dependent variable quantity is dimensionless
      iii. Source term quantity is none with units '1/s'
      iv. Dependent Variables
         1. Field name: *Vb_f*
         2. Number of dependent variables: 1
         3. Dependent variables: *Vb_f*
   b. Coefficient form PDE1
      i. Diffusion Coefficient, *c*: 0
      ii. Absorption Coefficient, *a:* 0
      iii. Source Term, *f* : *-r/rho_b*
      iv. Mass Coefficient, e_a : 0
      v. Damping or Mass Coefficient, d_a: 1
      vi. Conservative Flux Convection Coefficient, α : 0
      vii. Convection Coefficient, β : 0
      viii. Conservative Flux Source, γ : 0
   c. Zero Flux 1
   d. Initial Values 1
      i. Initial value for *Vb_f*: *Vb0_frac*
      ii. Initial time derivative of *Vb_f*: 0
9. Add Mass Source and Pressure nodes under Darcy's Law (dl)
10. Solving for the internal pressure using Darcy's Law
    a. Darcy's Law (dl)
       i. Equation
          1. Equation form: Study Controlled
          2. Show equation assuming: Study1, Time Dependent
       ii. Dependent Variables, Pressure: 'p'

        b. Fluid and Matrix Properties 1
            i. Equation
                1. Show equation assuming: Study 1, Time Dependent
            ii. Model Inputs
                1. Temperature, T: User Defined
                2. Absolute pressure, p_A: User Defined
            iii. Coordinate System Selection
                1. Coordinate System: Global coordinate system
            iv. Fluid Properties
                1. Fluid material: Domain material
                2. Density, ρ: User defined - '(p*M_gas)/R/T_furance'
                3. Dynamic viscosity, μ: User defined – 'mu'
            v. Matrix Properties
                1. Porous material: Domain material
                2. Permeability, κ: User defined – 'kappa'
                3. Porosity, ε_p: User defined – 'phi_inst'
    c. No Flow 1
            i. Show equation assuming: Study 1, Time Dependent
    d. Initial Values 1
            i. Initial Values, p: 'P_0'
    e. Mass Source 1
            i. Equation
                1. Show equation assuming: Study 1, Time Dependent
            ii. Mass Source
                1. Mass source, Q_m: 'r'
    f. Pressure 1
            i. Equation
                1. Show equation assuming: Study 1, Time Dependent
            ii. Pressure
                1. Pressure, p_0: 'P_0'

11. Creating an internal temperature gradient, Heat Transfer in Solids (if desired)
    a. Right-click Model1 > Materials and click Open Material Browser
            i. Select desired material(s) and their domain and click add material
    b. Right-click Heat Transfer in Solids(ht) and click Temperature
    c. Heat Transfer in Solids (ht)
            i. Select domains 1 & 2
            ii. Equation
                1. Equation form: Study Controlled
                2. Show equation assuming: Study1, Time Dependent
    d. Heat Transfer in Solids 1
            i. Equation
                1. Show equations assuming: Study1, Time Dependent
            ii. Heat Conduction
                1. Thermal conductivity, k: From material
            iii. Thermodynamics
                1. Density, ρ: From material

                2. Heat capacity at constant pressure, c_p: From material
          iv. Initial Values1
                1. Temperature, T: T_init
          v. Temperature1
                1. Temperature, T_0: 'T_furnace'

12. Mesh 1
    a. Size
        i. Calibrate for: General Physics
        ii. Predefined: Extremely fine
13. Modify the study settings under Study 1
    a. Step 1: Time Dependent
        i. Times: 'range(0,3,50000)'
    b. Physics and Variables Selection
        i. Coefficient Form PDE and Darcy's Law should have a green check under solve…
14. In Study1 > Solver Configurations > Time-Dependent Solver 1
    a. Time Stepping
        i. Method: BDF
        ii. Steps taken by Solver: Strict
        iii. Maximum BDF order: 5
        iv. Minimum BDF order: 1
15. Add a Stop Condition node under Study1 > Solver Configurations > Time-Dependent Solver 1
    a. Stop Condition
        i. Stop expression: 'Vb_stop'
16. Right click Study 1 and click compute

References

1. R. V. Shende and S. J. Lombardo, "Determination of binder decomposition kinetics for specifying heating parameters in binder burnout cycles," *J. Am. Ceram. Soc.* **85** [4] 780-786 (2002).
2. M. Salehi, "Kinetic Analysis of the Polymer Burnout in Ceramic Thermoplastic Processing of the YSZ Thing Electrolyte Structures Using Model Free Method," *Applied Energy* **95** 147-155 2012.
3. T. V. Lee and S. R. Beck, "A New Integral Approximation Formula for Kinetic Analysis of Nonisothermal TGA Data," *AIChE Journal* **30** [3] 517-519 (1984).
4. G Sivalingam, R Karthik and Giridhar Madras, "Kinetics of thermal degradation of poly(epsilon-caprolactone)," *Journal of Analytical and Applied Pyrolysis* **70** 631-647 3 A.D.
5. S. Zulfiqar and S. Ahmad, "Thermal degradation of blends of PVAC with polysiloxane - II," *Polymer Degradation and Stability* **71** 299-304 2001.
6. J. S. Reed, "Principles of Ceramics Processing 2nd Edition," 1995.
7. M. Barsoum, "Fundamentals of Ceramics," 1997.
8. D. J. Shanefield, "Organic Additives and Ceramic Processing, Second Edition: With Applications in Powder Metallurgy, Ink, and Paint," 1996.
9. S. P. Timoshenko and J. N. Goodier, "Theory of Elasticity Third Edition," 515-520 1970.
10. W. D. Callister and D. G. Rethwisch, "Materials Science and Engineering Eighth Edition," 9 2011.
11. C. L. Beyler, "Thermal Decomposition of Polymers," *The SFPE Handbook of Fire Protection Engineering* 165-178 1988.
12. J.-L. Dirion, C. Reverte and M. Cabassud, "Kinetic Parameter Estimation From TGA: Optimal Design of TGA Experiments," *Chemical Engineering Research and Design* **8** 618-625 2008.
13. L. C. K. Liau, B. Peters, D. S. Krueger, A. Gordon, D. S. Viswanath and S. J. Lombardo, "Role of length scale on pressure increase and yield of poly(vinyl butyral)-barium titanate-platinum multilayer ceramic capacitors during binder burnout," *Journal of the American Ceramic Society* **83** [11] 2645-2653 (2000).
14. A. C. West and S. J. Lombardo, "The role of thermal and transport properties on the binder burnout of injection-molded ceramic components," *Chemical Engineering Journal* **71** [3] 243-252 (1998).
15. J. W. Evans, "The Production of Inorganic Materials," 76-110 1991.
16. F. Moisy, "EzyFit 2.40," *http://www. mathworks. com/matlabcentral/fileexchange/10176* 2010.

Curriculum Vita

Matthew L. Incledon

Education:

2013 M.S., Materials Science and Engineering, Rutgers University

2011 B.A., Physics, Gettysburg College

Work Experience:

2011 – 2013 Graduate Research Assistant, Department of Materials Science and Engineering, Rutgers University